Master's thesis

NTNU
Norwegian University of Science and Technology
Faculty of Information Technology and Electrical Engineering
Department of Electric Power Engineering

Marius Moldestad

Evaluating pathways for hydrogen produced from low-carbon energy sources

Master's thesis in Energy and Environmental Engineering
Supervisor: Magnus Korpås
June 2020

NTNU
Norwegian University of Science and Technology

Marius Moldestad

Evaluating pathways for hydrogen produced from low-carbon energy sources

Master's thesis in Energy and Environmental Engineering
Supervisor: Magnus Korpås
June 2020

Norwegian University of Science and Technology
Faculty of Information Technology and Electrical Engineering
Department of Electric Power Engineering

NTNU
Norwegian University of
Science and Technology

Abstract

Drastic measures are required in the transformation of the European economy towards climate neutrality, and hydrogen is expected to play an integral part in the decarbonisation process, with a political climate growing in favour towards the expansion of hydrogen-based technologies.

This master's thesis has the objective to analyse the influence of large-scale deployment of hydrogen in a future European multi-energy carrier system. The analysis is conducted with the use of a least-cost capacity investment model developed for this purpose, which co-optimises investments in electricity generation and hydrogen production infrastructure. The model is applied to a developed scenario in 2050, comprising of the North Sea countries aggregated into nodes.

The main findings are that hydrogen produced from electrolysis is the dominant production pathway, with 65 % of the production share in the base scenario. The deployment of a CO_2 price of 60 €/t, favours CCS-based H_2 production from steam-methane reforming (SMR), constituting the remaining share. Storage facilities see high utilisation, as 30 % of the electrolytic hydrogen is transported via storage before consumption.

The combination of technology cost-reductions and hydrogen production integration effectuates deployment of large shares of onshore and offshore wind. The system flexibility provided by the integration of hydrogen production and storage in the energy system is found to increase the net share of renewable energy sources (RES) in the electricity mix from 63.5 % to above 70.9 %, reducing CO_2 emissions by 6 million tonnes.

Moreover, the CO_2 price is found to be highly influential of the energy and hydrogen production mix, as CCS-technology is introduced in power generation at 30 €/t CO_2, and in SMR between 30 and 60 €/t CO_2.

The average hydrogen production price is estimated between 1.57 and 2.6 €/kg, with price levels seen between 1 €/kg and 2.6 €/kg for varying future electrolyser and renewable energy costs.

The system is also found to be significantly impacted by natural gas prices, with a 38 % share of power generation from fossil fuels at a 50 % price reduction from the base case natural gas price of 11.5 €/MMBtu, with no CO_2 cost. The cost parity between electrolysis and SMR with CCS is found at a price natural gas price around 8.1 €/MMBTU with a CO_2 price of 60 €/t.

The study should be complemented with research of higher temporal and spatial resolution, considering additional hydrogen pathways, to provide more robust results.

Nonetheless, the findings indicate that integrating large-scale hydrogen production into the energy system can facilitate renewable energy penetration and that the deployment of a CO_2 price is a pivotal measure towards decarbonisation.

Sammendrag

Drastiske tiltak kreves for å transformere Europa mot klimanøytralitet, og hydrogen forventes å spille en viktig rolle i avkarboniserings-prosessen, med et voksende politisk klima i favør av hydrogenbaserte teknologier.

Denne masteroppgaven har som mål å analysere effekten av storskala integrering av hydrogen i et framtidig europeisk energisystem. Analysen er utført med hjelp av en investeringsmodell som minimerer kostnader relatert til investering i elektrisk- og hydrogeninfrastruktur. Modellen brukes på et utviklet scenario i 2050, bestående Nordsjølandene, som er inndelt i noder.

Hovedfunnene i oppgaven er at hydrogen produsert fra elektrolyse er den dominerende produksjonsmetoden, med en produksjonsandel på 65% i base case scenarioet. En CO_2-pris på 60 € /t favoriserer CCS-basert hydrogen fra naturgass (SMR), som utgjør den resterende andelen av hydrogenproduksjonen. Resultatene viser også høy lagringsutnyttelse, ettersom 30 % av hydrogenet produsert på elektrolyse går via lager før bruk.

Kombinasjonen av kostnadsreduksjoner for teknologier og integrering av hydrogenproduksjon bidrar til ekspansjon av onshore og offshore vind i systemet. Resultatene viser at systemfleksibiliteten som er gitt ved integrering av hydrogenproduksjon og lagring i energisystemet, øker nettoandelen av fornybare energikilder i elektrisitetsmiksen fra 63,5 % til over 70,9 %, noe som reduserer CO_2 utslipp med 6 millioner tonn.

Videre viser resultatene at CO_2-prisen er svært innflytelsesrik på energi og hydrogenproduksjonsmiksen, ettersom CCS-teknologi blir introdusert i kraftproduksjon til 30 € /t CO_2, og i SMR mellom 30 og 60 € /t CO_2.

Gjennomsnittlig produksjonspris for hydrogen er beregnet mellom 1.57 og 2.6 € /kg, med produksjonskostnader observert mellom 1 € /kg og 2.6 € kg for ulike kostnadsnivåer til fremtidige elektrolyse og fornybar energi teknologier.

Naturgassprisen er også funnet til å ha betydelig påvirkning på systemet, med 38 % andel av kraftproduksjonen fra fossile brensler ved en 50 % prisreduksjon fra base case naturgasspris på 11.5 € / MMBtu, uten CO_2 kostnad. Kostnadspariteten mellom elektrolyse og SMR med CCS er funnet til en naturgasspris på rundt 8.1 € / MMBTU med en CO_2-pris på 60 € /t.

For å gi mer robuste resultater bør masteroppgaven kompletteres med studier med høyere tidsmessig og detaljmessig oppløsning, og med ytterligere hydrogenproduksjonsmetoder.

Funnene indikerer imidlertid at integrering av storskala hydrogenproduksjon i energisystemet øker integreringen av fornybar energi og at bruken av en CO_2-pris er et sentralt

virkemiddel til avkarbonisering.

Preface

This work marks the end of an era. 3 years of studying Business Administration and 5 years of Energy and Environmental engineering, 8 in total, close to 60 exams and what feels like a million hours of reading, working, practising, has lead up to this point. I must say I am extremely proud of what I have learned, experienced, and in the end, achieved. Although the journey has been tough at times, I would not be the person I am today, had I chosen another path. I have heard many people say that the years they spent studying has been the best years of their life, and I can see what they mean. It has certainly been 8 eventful years, with many experiences and impressions. However, I must say, I am extremely excited to see what life has to offer for me next, and I am determined to keep learning and growing, to seek new experiences and meet new exciting people.

Many people, directly or indirectly, have contributed to this work.

First and foremost, I would like to thank my supervisor Magnus Korpås for helping me design such an exciting project. He has been extremely encouraging and motivating, and his guidance and support has been invaluable. I would also like to express my deepest appreciation and gratitude to my co-supervisor, Espen Flo Bødal, for the endless hours of assistance and work towards this thesis and for being a valuable discussion partner. Without him, none of this would have been possible.

Secondly, I would also like to thank my parents for their love and support through the years. Their encouraging words, endless help, no matter the situation, and not to say brilliant Sunday dinners, has been (and will continue to be) invaluable, and its safe to say I would not be where I am without them. I would also like to thank two brothers, Anders and Henrik, for always keeping it fun, for keeping me on my toes and for motivating me to keep growing. I am extremely excited and motivated by their development and accomplishments, and I must say I am proud to be their older brother.

Thirdly, I would like to thank my grandparents. My grandmother Asbjørg for her love and kindness, and considerations of my well-being. Without her numerous dinner invitations, this "Larvstaur" would go hungry. And my grandfather Jan M., for always taking an interest in my work, and for exciting discussions and support. I see many similarities between us, and in many aspects he represents the person I strive to become. He is truly a role model.

Lastly, I would like to thank all my friends for unforgettable memories and support thus far (if they ever read this, they will know who they are). A special appreciation towards my roommates and the people involved in "Bakis", for keeping the mood light, and for creating memorable moments in, what has been a strange, but exciting, semester.

“I have never tried that before, so I think I should definitely be able to do that.”

Astrid Lindgren, Pippi Longstocking.

Contents

List of Tables

List of Figures

Abbreviations

H_2	-	Hydrogen
TSO	-	Transmission system operator
ETM	-	Energy transport model
°C	-	Degree Celsius
TWh	-	Terawatt hours
NG	-	Natural gas
pp	-	Percentage points
GHG	-	Green house gas
CCS	-	Carbon Capture and Storage
CO_2	-	Carbon dioxide
AE	-	Alkaline electrolyser
OH^-	-	Hydroxide ion
MJ	-	Megajoule
CAPEX	-	Capital expenditures
OPEX	-	Operational expenditures
kW	-	Kilowatt
GWh	-	Gigawatt hours
GW	-	Gigawatt
CO	-	Carbon monoxide
LCOE	-	Levelised cost of electricity
Cp	-	Capacity factor
LP	-	Linear programming
LCOT	-	Levelised cost of transport
PV	-	Photovoltaic
O&M	-	Operation and maintenance
CT gas	-	Combustion turbine
CC gas	-	Combined-cycle gas
CO_2 e	-	Carbon dioxide equivalent
PEM	-	Proton exchange membrane
RES	-	Renewable energy sources
VRE	-	Variable renewable energy
SMR	-	Steam methane reforming
FCEV	-	Fuel cell electric vehicle
AIC	-	Annual investment costs
CRF	-	Capital recovery factor

Nomenclature

Indices

i	Plant type
n, m	Bus
t	Time step

Parameters

η	In/out efficiency for battery or hydropower
γ	Conversion factor for energy to hydrogen, directly or via storage $[MWh/kg]$
C_i^e	Cost of CO_2-emissions $[€/MWh]$ or $[€/kg]$
$C_n^{H_2ng}$	Cost of hydrogen from natural gas $[€/kg]$
$C_{i/y}$	Investment, variable, fixed, retirement or rationing cost $[€/MW]$ or $[€/MWh]$
D_{tn}	Electricity or hydrogen demand $[MWh]$ or $[kg]$
F_{tn}	Inflow, regulated or unregulated $[MWh]$
P_i	Max or min capacity of power plant $[MW]$
P_{tin}	Power profile $[MWh]$
R_i	Maximum ramping, up or down $[MW]$
T_{nm}^{max}	Maximum transmission capacity from bus n to m $[MW]$
X_{in}^{init}	Initial number of power plants

Sets

$\mathcal{C}_i$	Buses connected to bus i by transmission lines
$\mathcal{N}$	All buses
$\mathcal{P}, \mathcal{R}$	All power plants or renewable power plants
$\mathcal{S}$	All storage units
$\mathcal{T}$	Time steps

Variables

a_{tnm}	Power flow from bus n to m $[MW]$
b_{tn},b_n^{cap}	Energy to/from battery or battery capacity [MWh][MW]
c_{tin}	Energy curtailment of renewables $[MWh]$
e_{tn}, e_n^{cap}	Battery/hydro storage level or energy capacity $[MWh]$
f_{tn}	Energy from hydropower $[MWh]$
h_n^{cap}	Electrolysis capacity $[MW]$
h_{tn}	Hydrogen flow, directly to load, to or from storage and from SMR with or without CCS $[kg]$
$p_{ti}^{exp/imp}$	Power import or export $[MW]$
p_{tin}, r_{tn}	Power production or load curtailment $[MW]$
s_{tn}, s_n^{cap}	Storage level or capacity $[kg]$
u_{tin}	Committed power plants
x_{in}	New thermal and renewable power plants, new storage or retired power plants

Chapter 1

Introduction, motivation and background

1.1 Introduction

At the end of 2019, the European Commission (EC) launched its European Green Deal (EGD), meant to combat the challenges that are ahead in regards to environment and climate, and transform EU into a sustainable, resource-efficient and competitive economy. Current policies and actions are projected to achieve reductions of greenhouse gas emissions of around 45 % by 2030 and 60 % by 2050, which are insufficient to reach Paris Agreement-targets. With the EGD, the EC sets the ambition with a long-term vision to transform Europe into a climate-neutral economy by 2050, legislated by the first European "Climate Law" [1]. The EU is committed, in an Industrial Revolution-like manner, to radically transform its entire economic system, in just a matter of decades. Increasing the share of renewable energy in the power mix can contribute in the decarbonisation process of Europe, but all sectors must be expecting to change. The EDG means that drastic fundamental measures are required, and a paradigm shift in sectors such as agriculture, transportation, industry, power and buildings is inevitable if the objective is to be met. For example, transport accounts for a quarter of the EU's greenhouse gas emissions, consequently requiring a 90% reduction in transport emissions to achieve climate neutrality by 2050.

Employing an energy carrier whose characteristics enables use in a broad spectrum of applications, and which can coexist and synergise with the electric economy [2], can help accelerate the transition towards climate neutrality—namely hydrogen.

1.2 Motivation

Hydrogen (H_2) is the most abundant element in the entire universe and can be produced from a variety of low-carbon sources [3]. It offers a versatile and flexible energy vector in the transition towards climate neutrality, with no tailpipe emissions[4]. Utilising, for example, water electrolysis powered by renewable electricity to produce hydrogen means that the hydrogen can be close to emission-less over its entire life cycle [5]. Consequently, hydrogen can provide buildings, industries and the transportation with emission-free energy and feedstock, coupling sectors with the power-producing sector. It can also be utilised for long-term, large-scale storage, and provide flexibility and energy security to the energy system.

As discussed by [4], EU policies up till now have not directly supported the development of hydrogen. However, in March 2020, the European Commission launched its initiative, "A EU hydrogen strategy", specifically aiming to explore how clean hydrogen can contribute towards cost-effective climate gas emission mitigation and the objectives of the EGD, and establishing a mission to facilitate the integration of hydrogen at large towards 2050 [6].

1.3 Objective

On the basis of a favourable political climate towards the integration of a hydrogen economy in the EU, involving large-scale deployment of hydrogen-based technologies in 2050, this master's thesis seeks to analyse a future European energy system comprising of both electricity and hydrogen as energy carriers. The system constitutes of several European countries in 2050, all assumed to have incorporated hydrogen into their economies, and seeks to investigate:

- The development of a future power system integrated with hydrogen production
- The composition of production technologies for hydrogen
- The economics of producing hydrogen in an integrated system
- Implications of dynamic hydrogen production on renewable energy deployment
- Implications of exogenous factors, such as the price of carbon dioxide or natural gas, on hydrogen- and electricity production

The study expands the previous research of dynamic hydrogen production and optimisation, conducted in the project thesis leading up to this master's thesis [7], to a larger system, investigating hydrogen pathways from low-carbon energy sources in a greater context. Several studies of a European energy system penetrated by hydrogen have previously been conducted [4, 8, 9]. While these studies deviate from this thesis in terms of

methodology, input assumptions and resolution, they provide solid benchmarks of which the results from this work will be compared.

The structure of this master's thesis is as follows. Chapter 2 provides a brief overview of the applications of hydrogen, and hydrogen produced from electrolysis and natural gas. Chapter 3 describes the methodology used to build the capacity expansion optimisation model utilised in this thesis. Chapter 4 describes the input and assumptions for the 2050 European multi-energy carrier scenario subject to analysis. Results from the optimisation are provided and briefly commented in Chapter 5 before the findings are discussed in detail in Chapter 6. Chapter 7 provides the conclusion and further work.

Chapter 2

Hydrogen as an energy carrier

This section will briefly cover the use of hydrogen with an emphasise on the power sector, and the different production pathways.

2.1 Use of hydrogen

Hydrogen is not a source of energy itself, but rather an energy carrier. It is also known as an energy vector, as it can be used to convert, store and deliver energy. Hydrogen's high energy content and lightweight makes it applicable for various energy-intensive purposes, and it does not emit greenhouse gases or common air contaminants like sulphur or nitrogen oxides when used. Today, hydrogen is widely utilised in industrial processes such as oil refining, and as a chemical feedstock in the production of for example ammonia. However, it is expected to see more extensive use in various application and circumstances in the future. As seen from Figure 2.1, The Fuel Cells and Hydrogen Joint Undertaking (FCH JU) anticipate that hydrogen will play a role in power generation and buffering, transportation, heating and power for buildings, and industry energy the next decades [10].

According to FCH JU estimates, hydrogen could have a share as high as 24 % of the final energy demand, spread across the mentioned sectors in the EU by 2050, as the commitment to achieve the 2-degree scenario stated in the Paris Agreement will require structural changes to industries in terms of energy sources and feed stock. In a less ambitious "business as usual"-scenario, where no additional effort towards decarbonisation is made, hydrogen still sees significant employment compared to current practises.

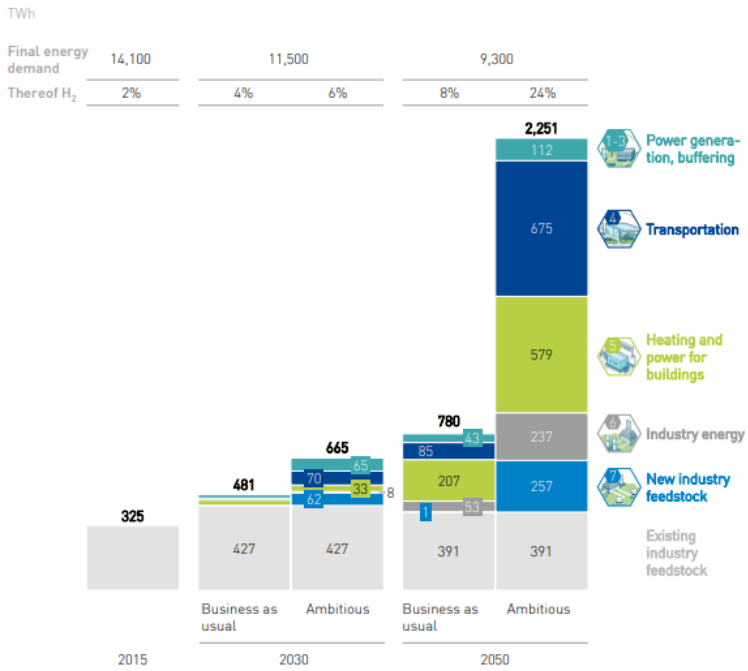

Figure 2.1: Hydrogen share of final energy demand and demand by sector in 2050 [10]

2.1.1 Transportation

Fuel cell electric vehicles (FCEVs) running on hydrogen produced from low-carbon sources provides a decarbonisation option for the mobility sector, as electricity, water and heat are the only by-products of a fuel cell. In the personal car segment, hydrogen must compete for market share with other low-carbon technologies like electricity or bio fuels, making cost the influential factor for the future balance between them. However, FCEVs are regarded as complementary to battery electric vehicles, providing driving range and fuelling time comparable to conventional vehicles. These characteristics, in addition to significantly higher volumetric and gravimetric energy density compared to batteries [10], makes hydrogen the superior option for heavy-duty transportation. Hydrogen can thus play an essential role in the decarbonisation of larger passenger cars, trucks, buses, trains and even maritime- and airborne transportation.

2.1.2 Industry

The industry sector accounts for most of the present hydrogen demand. It is widely utilised as a chemical feedstock in ammonia and polymers production and refining for hydrocracking and hydrotreating. It is also used to some extent in heat treatment in steel and iron production and other smaller areas of application such as semiconductors, cooling or as

rocket fuel. As the hydrogen used is almost exclusively based on fossil fuels, a switch to low-carbon hydrogen in these CO_2 emission-intensive processes can lead to significant emission reductions. The Norwegian steel producer Celsa recently revealed plans to use renewably produced H_2 to power their furnaces, aiming to fully decarbonise the company's production line within 2050 [11]. Furthermore, combustion of hydrogen can generate the high temperature heat required for gasification, melting or catalysation, thus replacing gas or coal with a low-emission alternative for energy intensive industries like aluminum, steel or cement. With significant potential quantities of hydrogen used as both industry feedstock and industry energy, the global industrial sectors could act as a strategic enabler for an immature electrolytic hydrogen market. This could facilitate economic scaling effects and following cost reductions, which could expedite further market growth and economics.

2.1.3 Buildings

Buildings account for about a third of the global energy consumption, where the majority is used for heating and warm water supply. Heating is mostly generated from natural gas, oil, coal or biomass, and buildings are consequently responsible for about 20 % of the emissions in the world today [12]. Substituting these fossil-based fuels with hydrogen from low carbon sources can thus significantly reduce GHG emissions. Hydrogen can be utilised both as fuel or as an energy converter in this context. Fuel cells can be used as small combined heat- and power plants, delivering efficiency above 90 % for heat and power [13]. Existing gas infrastructure can with only minor modifications and investments provide hydrogen-based fuel for combustion. This can fully or partially decarbonise building heating, and can possibly provide a more cost-competitive solution to infrastructure upgrades required for electric heating.

2.1.4 Power

In the power sector, hydrogen can expedite the transition from fossil fuel-based electricity to renewable. Hydrogen offers valuable advantages in this context, as it avoids CO_2 and particles emission, can be deployed at large scale , and can be made available everywhere. Hydrogen has several attributes making it desirable for operation in combination with renewable energy sources, such as high dynamics and modularity of electrolysers and related storage systems. It also provides a mechanism to flexibly transfer energy across sectors, time, and place, so-called sector coupling [14]. Hydrogen is expected to play a vital part in power system balancing, facilitating renewable energy integration and providing energy security.

Buffering

Increasing the use of electricity and of sources of varying nature in the power sector can put pressure on the power system, as large fluctuations in supply and demand can cause

system imbalances. [5] finds that the emergence of these situations are typical when variable renewable energy (VRE) constitutes about 25-30 % of the annual electric energy mix or above. In the power market, ancillary- or balancing services are applied to quickly neutralise such an event, adjusting the balance in the power grid in the short-term. Power producers can supply these services with options for swiftly regulating levels of generation or by large consumers with adjustable power consumption, for example, an aluminium producer. An increase in renewable power generation causes an increase in the need for flexible balancing power, which is more expensive than in the day-ahead markets due to the cost-of-readiness [15]. A hydrogen system with fuel cells, electrolysers and built-in storage capacity can be used as a buffer to meet the need for these services in a more cost-efficient way. Hydrogen production, and hence the electricity consumed by the electrolyser, can be adjusted quickly to provide balancing power to the system in real-time. Power buffering services can thus provide an additional source of income for electrolysers and as a consequence, lower the cost of hydrogen [16]. On the contrary, fuel cells can use built-up hydrogen storage to supply balancing power quickly. Increasing the financial competitiveness of electrolyser by exempting them from grid charges could be a tool to encourage electrolyser deployment for ancillary services.

Energy security

Hydrogen can also be utilised as a more long-term medium for electric energy storage. While batteries and demand-side measures, such as flexible electrolyser operation, can be used for short-term buffering, these options inadequate to provide security of power supply over longer time frames [10]. The long duration of hydrogen-based energy storage system makes it a promising option for seasonal storage of electricity for countries with high shares of VRE capacity [17, 18], accumulating energy to storage at periods of oversupply with electrolysis, while providing energy at times of insufficient supply via fuel cells. However, the conversion of electricity and reconversion of hydrogen results in a low round trip electrical efficiency of about 40 % [5], and the value-added by this type of storage system and its economic viability remains unclear at this stage [17].

Grid investments and renewable energy integration

Massive grid infrastructure investments and upgrades are required to accommodate increasing shares of renewable power production. Replacing electricity with hydrogen as the energy carrier can reduce the need for grid infrastructure investments, as hydrogen enables long-distance transportation of energy with minimal losses. Renewably produced hydrogen can be exported from site by ships, trucks, trains or in pipelines, providing a lower-cost alternative to power grid transmission in some cases. For areas of particular geographical remoteness or technical conditions, hydrogen conversion, storage and transport can enable and increase the exploitation of the energy source, and deliver cheap renewable energy to regions with limited production or higher cost of power generation [19]. Using hydrogen for energy conversion and transportation can thus accelerate the deployment

of renewable energy as the bottle-neck of constrained transmission is circumvented. The operational flexibility provided by a H_2 system can also make renewable energy integration more cost-effective, as it can be used to optimise power exchange between a variable power source and the electricity grid, facilitating a more efficient penetration of power generation technologies with congested power grids [20].

2.2 Hydrogen production

Figure 2.2 shows the different production pathways for hydrogen. The production methods comprise of electrolysis, biochemical conversion of algae or biomass, and thermochemical conversion processes, such as steam methane reforming (SMR), partial oxidation and autothermal reforming. Hydrogen produced by electrolysis or biomass is usually referred to as green hydrogen, as long as the related emissions are lower than 8 kg CO_2 e/kg H_2 throughout its entire life cycle [5]. Grey hydrogen refers to hydrogen produced from fossil sources like natural gas, oil or coal via thermochemical conversion. When adding carbon capture and storage (CCS) to the production process from fossil sources, the output is referred to as blue hydrogen. This section will focus on two prominent paths, hydrogen produced from SMR of natural gas and electrolysis.

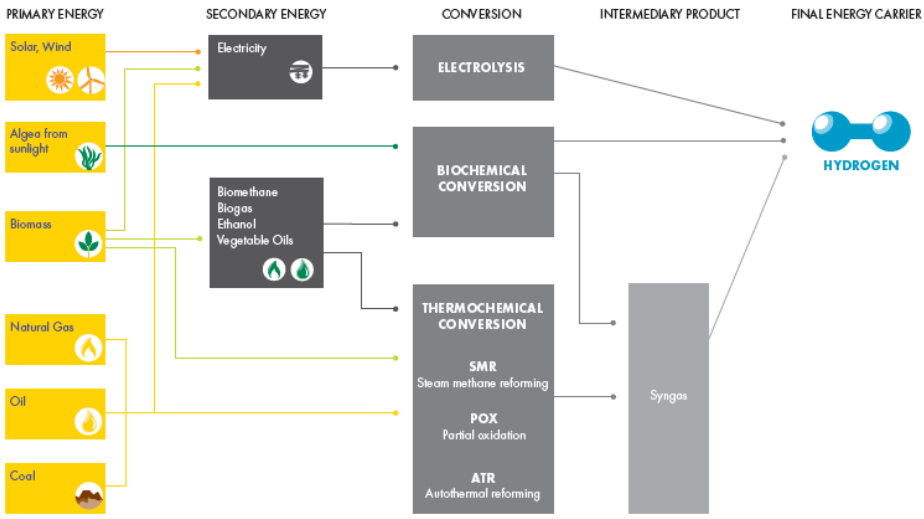

Figure 2.2: Processes for producing hydrogen [3]

2.2.1 Natural gas

Today, the most widespread hydrogen production pathway is by steam methane reforming of natural gas, constituting approximately 75 % of the annual hydrogen production [14]. To produce hydrogen from SMR, natural gas and water is used as input, and the methane (CH_4) contained by natural gas is reacted with steam, as seen from Equation 2.1, at the presence of a catalyst. The reaction is endothermic, requiring temperatures of 700-1000 °C, which is supplied by an integrated furnace driven by natural gas and tail gas from the SMR process [21]. The steam reforming reaction produces carbon monoxide (CO), in addition to H_2, which is subsequently reacted with steam in what is called the water gas shift reaction. The water-gas shift, seen in Equation 2.2, produces a synthetic gas consisting of H_2 and CO_2. Small amounts of residual CH_4 and CO are also present. A process called pressure swing adsorption is then used to remove CO_2 and other impurities to deliver hydrogen at a purity of 99.9 +% [22].

$$CH_4 + H_2O \Rightarrow CO + 3H_2 \tag{2.1}$$

$$CO + H_2O \Rightarrow CO_2 + H_2 \tag{2.2}$$

Today, this process occurs in large centralised plants, and produces the cheapest available hydrogen in the market, at levels as low as 0.85 €/kg, depending on the geographical location of production [14].

Low carbon hydrogen from SMR

The conversion of natural gas to hydrogen with SMR produces considerable amounts of CO_2 as a by-product, with today's SMR technology releasing around 9–11 kg CO_2 per kg H_2 [21]. Consequently, as most of the hydrogen produced today stems from fossil sources, considerable emissions are produced. Carbon capture and storage can be utilised in 3 steps, as shown in Figure 2.3, to remove the substantial shares of CO_2 from the production process. This is found to reduce the CO_2 emissions up to 90 % today, with capture rates above this level expected in the future [14].

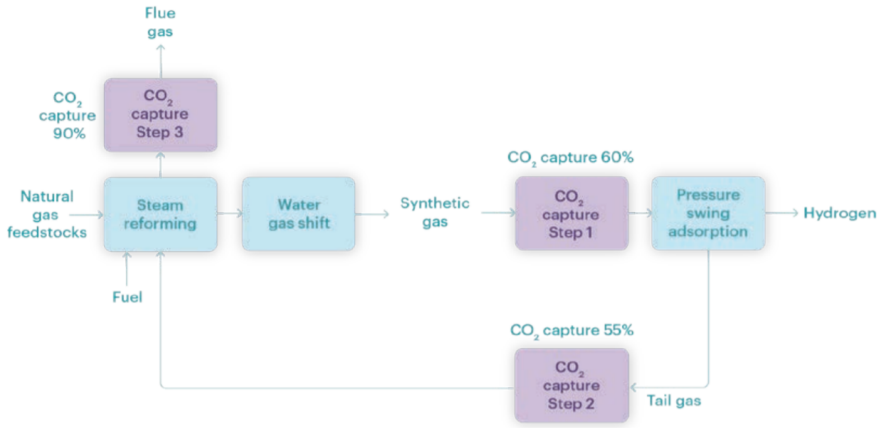

Figure 2.3: The hydrogen production process from SMR with CCS [14]

2.2.2 Electrolysis

Electrolysis is an electrochemical process which uses electricity to convert water molecules to hydrogen and oxygen. Figure 2.4 depicts the hydrogen production process in a proton-exchange membrane (PEM) electrolyser.

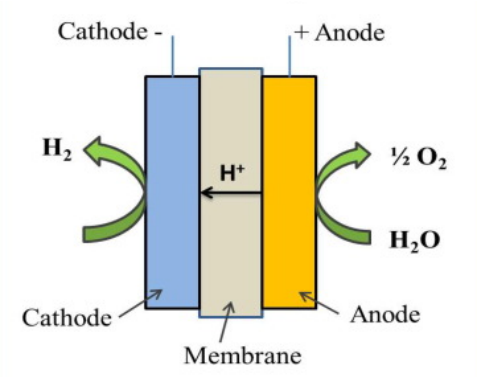

Figure 2.4: PEM electrolysis [23]

It consists of two electrodes, an anode and a cathode which are separated by an electrolyte, in this case, a proton-conducting membrane (also called polymer electrolyte membrane). Water is supplied to the electrolyser anode, where it is split into hydrogen, oxygen and electrons (e^-) , as seen from Equation 2.3. The H^+-protons move from the anode through the membrane, while the electrons travel via an external power circuit connected to a direct current source, to the cathode, recombining with H^+ to produce H_2, as shown in Equation

2.4 [23].

$$H_2O \Rightarrow 2H^+ + 1/2O_2 + 2e^- \tag{2.3}$$
$$2H^+ + 2e^- \Rightarrow 2H_2 \tag{2.4}$$

There are various types of electrolysers in the market today, differentiated by their electrolyte and operational temperature. However, this study focuses on PEM technology. The PEM electrolyser has a compact and easily scalable system design, and high dynamic operation with quick response, making it advantageous in a system with large shares of VREs. It also has significant hydrogen production rate and can produce hydrogen with a purity of 99.99 %, at energy efficiencies between 80-90 % [23].

Electrolysis only has a 0.1 % share of the dedicated hydrogen production globally today [14]. However, this is expected to change. [24] highlight that PEM electrolysers can reach costs below 400 €/kW by 2030, from above 1000 €/kW today, significantly lowering the production cost of hydrogen from electrolysis. Moreover, [3] estimates that water electrolysis can produce hydrogen with emissions of 13 g CO_2 /MJ H_2, or about 1.5 kg CO_2/kg H_2, provided that the electrolyser is supplied with electricity stemming from renewable energy sources (RES). As seen from Figure 2.5, this is about one-tenth of the emissions from SMR. However, using the current EU electricity mix doubles the emissions from electrolysis compared to SMR.

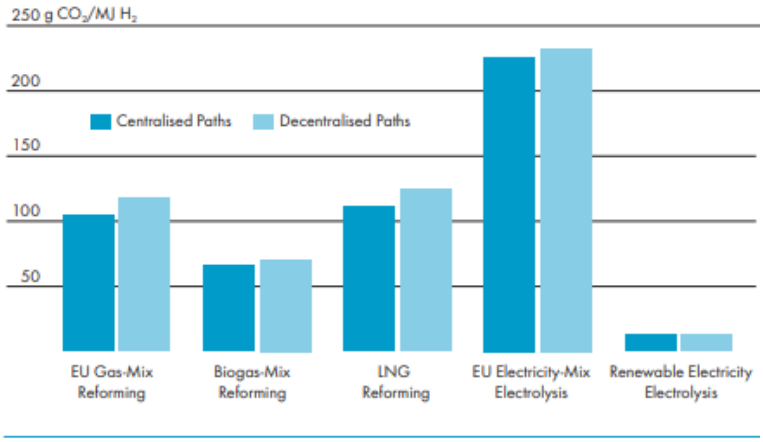

Figure 2.5: Emissions from hydrogen production [23]

The combination of cost reductions in electrolysers, and renewable energy generation technologies, and the low carbon footprint of the output hydrogen is expected substantially elevate the share of electrolytic hydrogen in the future hydrogen production mix.

Chapter 3

Method

This section will the describe capacity expansion modelling and the methodology used to build the optimisation algorithm and model.

3.1 Modelling

Previous studies use classic methods such as levelised cost of electricity (LCOE) calculations to investigate the economics of large-scale hydrogen production using low carbon energy [8, 25]. The previous research performed in the project thesis, providing some of the basis for this master's thesis, partly utilised an LCOE approach to evaluate hydrogen production from local wind and solar resources in Norway and Germany [7]. The LCOE approach can be used to compare costs of producing electricity from different technologies independently before the LCOE is then used to calculate hydrogen production costs based on assumptions of, e.g. a constant electrolyser capacity factor. While this approach can provide a basic overview and baseline for comparison of hydrogen production from different sources, it fails to consider important factors that exist and interact within the entire power generation system at large.

The varying nature of the electricity demand and integration of large shares of variable renewable energy sources with fluctuating capacity factors are highly influential on the electrolyser production rate. For example, [26] finds that dynamic use of energy storage options lowers the production costs of hydrogen. The project thesis and [16] both conclude that hydrogen produced flexibly using grid-electricity in combination with production from VRE and storage utilisation reduces production costs. Applying a constant electrolyser capacity factor and neglecting storage and power system dynamics can thus lead to inaccurate results. This master thesis aims to provide more realistic results from investigating large-scale hydrogen production by utilising optimisation modelling with a

capacity expansion approach to directly model electric power system and electrolyser operation.

3.1.1 Optimisation and linear programming

Optimisation modelling uses mathematical methods to find the best alternative in decision-making situations. The objective for the model is to optimise a stated quantity, by either minimising or maximising an objective function f(x) depending on various decision variables. This thesis formulates a cost-minimising problem as shown in Equation 3.1.

$$\begin{aligned} &\min f(x) && \\ &\quad s.t.\ \ g_i(x) \leq b_i && \forall i \in I \end{aligned} \tag{3.1}$$

The objective function f(x) is subject to constraints, where $g_i(x)$ are functions depending on x, and b_i are given parameters for all i in the set I [27]. In the context of energy models, the objective can be to optimise the power flow between nodes or investments in generation assets. These energy models are underlain an objective function seeking to, for example, minimise investment cost or power losses, or maximise welfare or profits. The objective function is subject to a set of constraints that reflect requirements to fulfil or physical realities, such as an energy demand in a bus, energy balances or congested power transmission lines.

This thesis utilises linear programming, a type of mathematical programming, to determine the optimal solution subject to linear relationships. This require all functions f(x) and $g_i(x)$ to be linear and that all variables x are continuous, and can be formulated as Equation 3.2.

$$\begin{aligned} &\min \sum_{n \in \mathcal{N}} c_p x_p && \\ &\quad s.t.\ \ a_{ij} \leq b_i && \forall i \in I \forall j \in \mathcal{J} \\ &\quad x_j \geq 0 && \forall j \in \mathcal{J} \end{aligned} \tag{3.2}$$

After the optimisation problem is formulated, the model uses a solution algorithm to find the optimal solution. Here, the simplex algorithm is applied to optimise a linear objective function subject to a linear system of constraints. The flow-chart of the simplex algorithm is depicted in Figure 3.1.

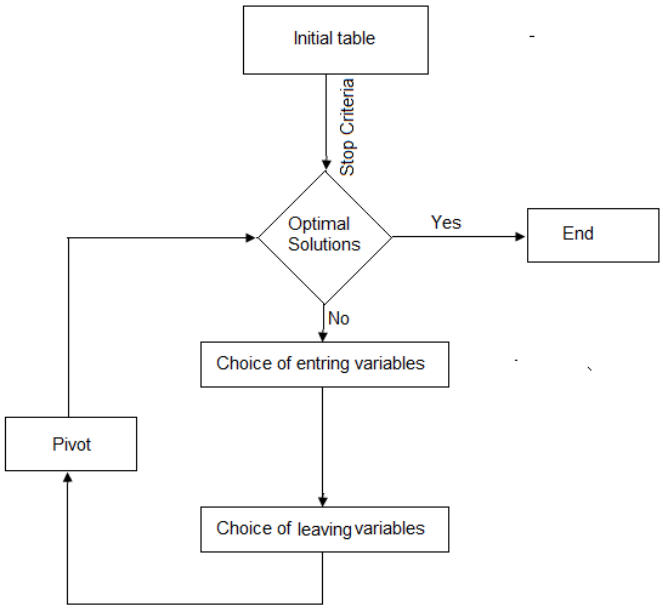

Figure 3.1: Flow chart of the simplex algorithm [28]

The optimal solution is determined by first finding a feasible solution to the problem. This solution is then iterating upon until the most favourable outcome is found [28].

Capacity expansion modelling

In this study, capacity expansion planning is used as the optimisation approach to evaluate pathways for hydrogen from low-carbon sources. This approach determines the most optimal mix of investments in energy-producing assets, subject to factors such as energy demand, fuel prices, technology cost and performance. This type of modelling is used by various professional entities, such as The National Renewable Energy Laboratory (NREL), to, for example, forecast impacts of policies and regulations of the electricity system and renewable energy expansion [29]. It has also been utilised in multiple previous studies involving assessment of low-carbon energy production and energy system planning [4, 9, 16, 30, 31, 32].

Capacity expansion planning can be used to for example

- Quantify the influence of various policy implementations on the energy mix
- Determine cost implications of alternative pathways to a carbon-neutral society
- Impacts of future prices of fossil fuels on renewable energy expansion

- Optimal grid infrastructure investments for integration of renewable technologies

In this case, the capacity expansion model will provide the optimal future investment structure in new power generating capacities to serve future electricity and hydrogen demand at the lowest possible cost.

3.1.2 Energy transport modelling

Various approaches exist for modelling power infrastructure into optimisation planning models, which can greatly impact model accuracy and computational time. In this thesis, an energy transport model (ETM), which considers the location of production and consumption of electricity, and power system dynamics, is used. This modelling approach is used in other capacity expansion studies and assumes that electricity is exchanged between the system nodes as an ordinary commodity [30]. The exchange of electricity is governed by Kirchhoff's current law, stating that the sum of electricity generation and import at each node must equal the sum of electricity consumption and export. Transfer capacities of the transmission grid regulate the maximum power flow between the nodes. Moreover, line losses are not considered in this thesis, as the primary purpose is to investigate the implications of hydrogen employment in the energy system rather than transmission loss dynamics. Furthermore, while other approaches, for example, the DC power flow approximation [33], allows for more realistic grid modelling, this increases both complexity and computational time. ETM provides a simplified way of modelling the electricity grid, while providing power system operation realistic enough for the purpose of this master's thesis, and is thus considered the best approach.

3.2 Multi-energy carrier optimisation model

The model implemented in this thesis is working on a multi-energy carrier system, with hydrogen production, flow and consumption in addition to electricity. It optimises capacity expansion planning of power generating assets and storage facilities, optimal generation dispatch, storage utilisation, and optimal power flow between system nodes. The model is created in cooperation with co-supervisor Espen Flo Bødal, and is based on previous works and research concerning his doctoral degree [16, 34], which is tailored for the purpose of this thesis. The optimisation algorithm is implemented in Python, an object-oriented programming language [35], and utilises the Pyomo optimisation language as the Python optimisation modelling tool [36, 37]. The Gurobi optimiser serves as the mathematical optimisation solver in the model [38].

The following sub-sections will describe the mathematical formulation of the hydrogen optimisation model created for this purpose. The model is formulated as a linear programming (LP) problem, as stated in Equation 3.3 to 3.21. The Nomenclature containing the relevant indices, parameters, sets and variables, is listed in the beginning.

3.2.1 Objective

The overall objective of the capacity expansion model is to find the most cost-effective composition of power- and hydrogen generating assets to meet future electricity and hydrogen demand in a bus. The objective function in Equation 3.3 minimises costs related to investment, retirement, fixed and variable operational costs for all power plant types, $\forall i \in \mathcal{P}, \mathcal{R}$, and storage units, $\forall y \in \mathcal{S}$, for all nodes, $\forall n \in \mathcal{N}$, for all times , $\forall t \in \mathcal{T}$. Consequently, the sum of all individual investments in renewable and thermal power, electrolysis, hydrogen or battery energy storage make up the total investment costs.

$$\begin{aligned}\min \sum_{n\in\mathcal{N}} \Big[& \sum_{i\in\mathcal{P}} (C_i^{inv} x_{in} + C^{ret} x_{in}^{ret} + C_i^{fix}(X_{in}^{init} + x_{in} - x_{in}^{ret})) + \\ & \sum_{i\in\mathcal{S}} (C_i^{en} s_{in}^{cap} + C_i^{pow} e_{in}^{cap}) + \\ & + \sum_{t\in\mathcal{T}} \Big[\sum_{i\in\mathcal{P}} (C_i^{var} + C_i^{emis}) p_{tin} + \sum_{n\in\mathcal{N}} \Big((C_n^{smr} + C^{emis}) h_{tn}^{smr} \\ & + (C_n^{smr+ccs} + C^{e}) h_{tn}^{smr+ccs} + C^{rat} r_{tn} \Big) \Big] \Big] \end{aligned} \tag{3.3}$$

Investment and fixed costs, C^{inv}, C^{fix}, C^{pow} and C^{en}, constitute the capital expenditures (CAPEX) associated with power generating assets, electrolysers and storage facilities. Costs of retiring an asset C^{ret} in the period is also included. The operational expenditures C^{var} comprise of variable operational costs stemming from variable O&M costs and fuel costs. Furthermore, CO_2-emission cost are considered for thermal power generation at a price C^{emis}. Hydrogen that is not produced by electrolysis using electricity can be supplied by steam methane reforming of natural gas at a given cost C^{smr} at each node with a related CO_2 emission. The emissions of hydrogen production from natural gas can be reduced by adding CCS, which will increase the levelised hydrogen production cost from SMR [14]. The cost of hydrogen from natural gas differs between the nodes in the system, due to the added cost related to the transmission of hydrogen produced by natural gas predetermined locations. Hence, hydrogen transport is indirectly modelled as opposed to electricity transmission, which is directly modelled. Lastly, unserved electricity demand is associated with a rationing penalty C^{rat}.

The operation of the system is governed by equations 3.4-3.21 for all times, $\forall t \in \mathcal{T}$, and all nodes , $\forall n \in \mathcal{N}$.

3.2.2 Energy balances and storage modelling

A schematic illustration of the two different energy balances for an arbitrary bus in the system is shown in 3.2.

A constant daily hydrogen demand in the node is supplied by hydrogen either produced

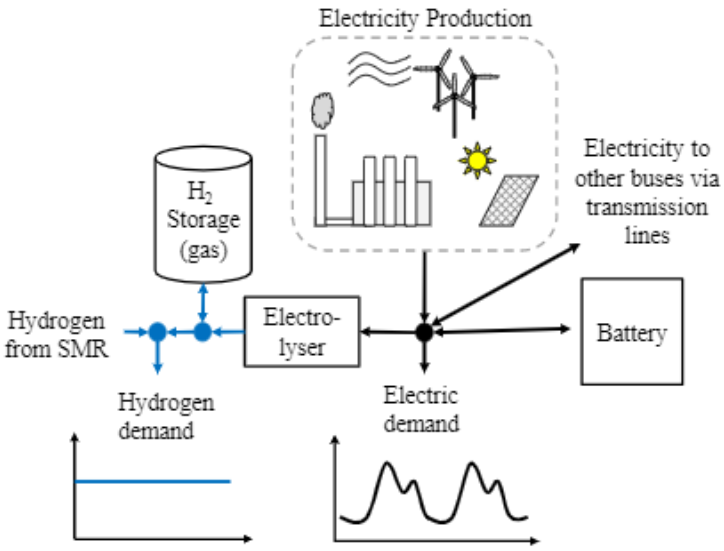

Figure 3.2: Schematic illustration of the two different energy balances for a bus in the system

from SMR or electrolysis. The algorithm can choose to invest in storage, which will allow for storage of hydrogen from the electrolyser, which can then be drawn upon to serve the hydrogen load at a later time stage. The electrolyser uses electricity to produce hydrogen. Each node also has a varying electricity demand which must be supplied. The algorithm must thus serve two electricity demands, demand from the electrolyser and local electricity demand. This electricity demand is either supplied from electricity production from local resources or from electricity imported through the transmission grid. As for hydrogen, there is an option to invest in storage, but in the form of batteries. Batteries used as electricity storage opens up for more flexibility to serve the two loads, as power produced can be stored for later use. In summary, the multi-energy carrier system thus requires equations to govern production, demand, import, export and storage utilisation for both carriers.

Electric energy balance

The electric energy balance at the buses are as stated in Equation 3.4, where injected energy from production p_{tin} or import p_{tn}^{imp} is balanced against extracted energy to serve electric load, export and hydrogen production. Energy can be stored and used to serve energy loads at a later time-stage. Electric energy can be sent to, b_{tn}^{out},- or withdrawn from, b_{tn}^{in}, battery storage, while hydrogen can be produced and sent via hydrogen tanks at an efficiency γ^{in}. Electricity can be converted to hydrogen for serving the hydrogen load directly, at a higher efficiency, avoiding storage pressure compression. Unserved electric demand is represented by demand rationing r_{tn}.

$$\sum_{i \in \mathcal{P}} p_{tin} - p_{tn}^{exp} + p_{tn}^{imp} + r_{tn} + \\ + b_{tn}^{out} - b_{tn}^{in} - \gamma^{dir} h_{tn}^{dir} - \gamma^{in} h_{tn}^{in} = D_{tn}^{El} \tag{3.4}$$

Electric storage

The battery storage balance is governed by Equation 3.5, which state that the energy stored in the batteries in a node n at time t, e_{tn}, is given by the sum of energy stored in the batteries at the preceding time-stage $e_{(t-1)n}$ and the net energy input into the battery with efficiencies η^{in} and η^{out}. The storage capacity at the node, e_n^{cap}, governs the maximum allowed storage level in Equation 3.6. The rate at which the battery can charge and discharge is given by the power capacity of the battery in Equation 3.7 and 3.8.

$$e_{tn} = e_{(t-1)n} + \eta^{in} b_{tn}^{in} - (1/\eta^{out}) b_{tn}^{out} \tag{3.5}$$
$$e_{tn} \leq e_n^{cap} \tag{3.6}$$
$$b_{tn}^{out} \leq b_n^{cap} \tag{3.7}$$
$$b_{tn}^{in} \leq b_n^{cap} \tag{3.8}$$

Hydrogen balance and storage

Similar to the load balance for electric power, we have a load balance for hydrogen, given in Equation 3.9. The daily hydrogen demand at a system node, $\mathrm{D}_{tn}^{H_2}$, is supplied directly from electrolysis, h_{tn}^{dir}, from storage h^{out} or from natural gas h_{tn}^{smr} and $h^{smr+ccs}$. Hydrogen produced from electrolysis can be stored locally in a hydrogen storage facility at each node, where the storage level is governed by the hydrogen storage balance in Equation 3.10, in a similar fashion as the battery storage balance. Equation 3.11 makes sure that the storage level e_{tn} does not exceed the maximum storage level. As hydrogen can be produced sent to storage or directly to the load, Equation 3.12 makes sure the sum of the electricity used for hydrogen production does not surpass the electrolyser capacity h_n^{cap}.

$$h_{tn}^{dir} + h_{tn}^{out} + h_{tn}^{smr} + h_{tn}^{smr+ccs} = D_{tn}^{H_2} \tag{3.9}$$
$$s_{tn} = s_{(t-1)n} + h_{tn}^{in} - h_{tn}^{out} \tag{3.10}$$
$$s_{tn} \leq s_n^{cap} \tag{3.11}$$
$$\gamma^{dir} h_{tn}^{dir} + \gamma^{in} h_{tn}^{in} \leq h_n^{cap} \tag{3.12}$$

3.2.3 Energy production modelling

Thermal power modelling

Equation 3.13 states that power plants available for operation must be less than or equal to the sum initially installed power plants X_{in}^{init} and capacity investments x_{in} less retired capacity x_{in}^{ret}. The minimum and maximum production limits P_i^{min} and P_i^{max} for thermal power technologies i, are governed by Equation 3.14. Equation 3.15 describes how thermal power plants are curbed by ramping constraints, restricting the rate at which production can be ramped up or down, R_i^{up} and R_i^{down}, between time periods t and t-1.

$$u_{tin} \leq X_{in}^{init} + x_{in} - x_{in}^{ret} \qquad \forall i \in \mathcal{P} \qquad (3.13)$$

$$P_i^{min} u_{tin} \leq p_{tin} \leq P_i^{max} u_{tin} \qquad \forall i \in \mathcal{P} \qquad (3.14)$$

$$-R_i^{down} u_{tin} \leq p_{tin} - p_{(t-1)in} \leq R_i^{up} u_{tin} \qquad \forall i \in \mathcal{P} \qquad (3.15)$$

Variable renewable energy modelling

Variable renewable energy production is governed by Equation 3.16. The production equals the input hourly power profile P_{tin}, providing the energy produced per unit power, for all renewable technologies $\forall i \in \mathcal{R}$, for all times $\forall t \in \mathcal{T}$, times the initial plants and investments in new renewable production capacity, for all nodes $\forall n \in \mathcal{N}$. The left side of the equation states that available renewable energy production is either used for producing electricity or it is disposed through curtailment, and that energy production must equal the sum of the two.

$$p_{tin} + c_{ti} = P_{tin}(X_{in}^{init} + x_i^{renewable}) \qquad \forall i \in \mathcal{R} \qquad (3.16)$$

Hydropower modelling

Due to its site-specific needs, the algorithm is prohibited from investing in new hydropower capacity, governed by Equation 3.17. With no new capacities in hydropower, the existing hydropower plants in each node are modelled as energy storage units, shown in Equation 3.18. The storage level e_{tn}^{hydro} at each node is determined by regulated and inflows F_{tn}^{reg} and F_{tn}^{unreg}, based on node-specific inflow data, less flow out, f_{tn}^{out}. As unregulated inflows are uncontrollable, Equation 3.19 states that the minimum production from a hydropower plant at node n must be larger or equal to the unregulated inflow, at time t.

$$x_n^{hydro} = 0 \tag{3.17}$$

$$e_{tn}^{hydro} = e_{(t-1)n}^{hydro} + F_{tn}^{reg} + F_{tn}^{unreg} - (1/\eta^{hydro}) f_{tn} \tag{3.18}$$

$$F_{tn}^{unreg} \leq f_{tn} \tag{3.19}$$

3.2.4 Transmission and power flow

Equation 3.20 governs power exchange between the system nodes. The power exported from the bus, p_{tn}^{exp}, less the power imported to the bus, p_{tn}^{imp}, equals the sum of the power flow on all transmission lines connected to the bus. Transmission losses are neglected, as an energy transport model is applied for this thesis. Moreover, the model is prohibited from expanding transmission capacity between nodes. Thus, the power flow on a transmission line is bounded by the maximum possible transmission capacity, T_{nm}^{max}, of the existing lines, as seen in Equation 3.21.

$$p_{tn}^{exp} - p_{tn}^{imp} = \sum_{m \in C_n} a_{tnm} \tag{3.20}$$

$$a_{tnm} \leq T_{nm}^{max} \qquad \forall m \in C_n \tag{3.21}$$

Chapter 4

Case study and input assumptions

This section will present the data and input assumptions used to create the 2050 hydrogen scenario base case simulated with the optimisation algorithm.

4.1 System

This master thesis investigates an integrated multi-energy carrier system constituted by the countries shown in Figure 4.1. The system is comprised of the countries bordering the North Sea; the Nordics, the UK, Ireland, Germany, the Netherlands and Belgium.

The countries subject to analysis are divided into bidding areas, where each bidding area is regarded as one centralised node. The bidding areas are used to indicate transmission system constraints, as the flow of power between different geographical location depends on the available transmission capacity between them. Thus, different bidding areas make sure that regional market conditions are reflected in the price of electricity, also referred to as the area price [39]. In the Nordics, the division of these areas is decided by the local transmission system operators (TSOs). Norway is divided into five bidding areas, Sweden into four and Denmark into east and west, while Finland is regarded as one area. The United Kingdom is assumed initially to be one price area. In this study, the UK is split into a northern, middle and southern price area on the basis of research conducted by Steve Voller, Associate Professor at the Department of Electric Power Engineering at NTNU [40]. Northern Ireland, Belgium and the Netherlands are regarded as one node each. Germany is also assumed as one single bus, as the entire country is subject to equal power prices. However, it is debated whether Germany will be divided into two price areas in the future. Production oversupply in the north and production scarcity in the south has created an energy imbalance, as transfer capacity between them are insufficient. Transfer capacity expansion is expected to be slow, and two bidding areas is argued to even out the

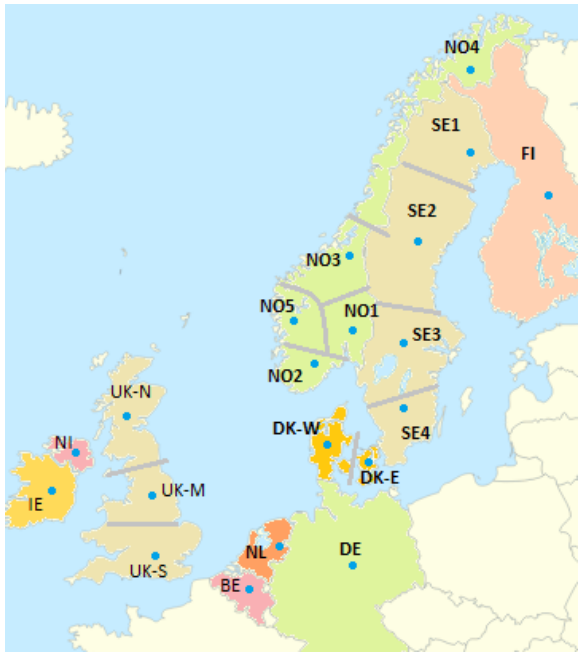

Figure 4.1: The areas investigated in the study

discrepancies between over- and undersupply between the regions [41]. However, such a discussion is outside the scope of this project. Hence, Germany is regarded as one bidding area for the sake of simplicity. The area division results in twenty nodes spread over ten countries.

4.2 Power system evolution

Power generation to serve electricity and hydrogen demand in the model derive from the input power production asset capacities expected in 2050 and capacity expansions by the model. The model hence requires estimates on the expected power generation capacities towards 2050 in the respective nodes. The data input used to predict power system evolution and build a 2050 base case is provided by Steve Völler. The data sets serve as the input for installed generation capacities, generated energy and consumption for each node. These data sets have previously served as the basis for research involving electrification of offshore oil and gas installations on the Norwegian continental shelf [40]. The data is sourced mainly from The "EU Reference Scenario 2016" (EUREF16) by the European Commission [42], research that has provided the benchmark for various policy implementations in the EU. The study provides a possible future energy scenario for the European energy system, describing the development for each of the 28 EU member states until 2050 in detail. Furthermore, as non-EU countries such as Norway are not included

in EUREF16, the remaining data are sourced from NTSO-E's "Ten Year Network Development Plan 2010" [43]. Both sources provide data on a country-level. Hence data are distributed into the respective nodes for countries represented with multiple buses, based on the approach used by [40].

The base case installations of each power generation technology regarded in this study, for each bus in 2050, are summarised in Table 4.1. The main sources of power in the 2050 base case are natural gas, onshore and offshore wind, solar PV, nuclear and hydropower. Lignite is phased out, while coal is, to a large extent, phased out, leaving gas as the dominant fossil fuel represented in the generation capacity mix. As seen in Figure 4.2, combined-cycle gas is expected as the largest power sources in terms of installed capacity in 2050. Onshore wind is expected to be the largest renewable source, slightly larger than offshore wind and solar PV.

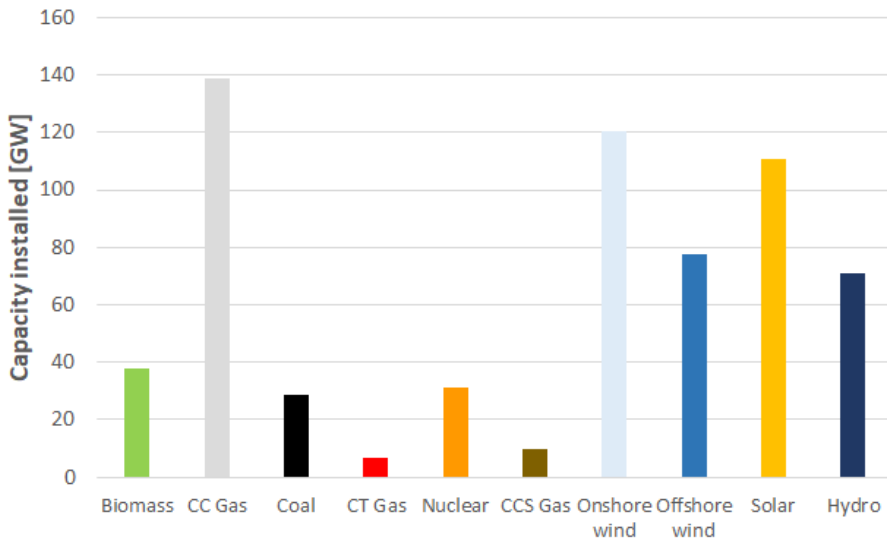

Figure 4.2: Total installed capacity for each power production technology in 2050

The input data involve several simplifications and assumption to reduce the number of input parameters, hence complexity and computational time. Firstly, gas power plants are represented by two types, combined-cycle gas (CC gas) and combustion turbine gas (CT gas), as other types of gas power plants have relatively low shares of installation. CC gas can be utilised to provide power for both base loads and perform decently at rapid fluctuations in demand with today's technology. Thus, open-cycle peaking plants are neglected [44]. It operates at higher efficiencies compared to CT gas due to the utilisation of excess heat from the gas turbine in a steam turbine, elevating the efficiency. Secondly, combined heat- and power plants, which mainly produce heat as output, are excluded, as determining their contribution to electric energy production in the system requires extensive research. Previous studies also neglect these plants [9, 30]. Lastly, other energy sources, such as coal with CCS or tidal power, are excluded from the scenario, due to minimal installation

in 2050.

Table 4.1: Expected installation of generation capacities in each node in 2050, given in GW [40, 42]

Bus	Bio	CC Gas	Coal	CT Gas	Nuc-lear	CCS Gas	Ons Wind	Off Wind	Solar	Hydro
BE	1.0	14.8		0.7			9.5	4.9	5.7	0.2
DE	6.6	41.4	24.0	1.7		7.9	57.4	28.6	86.9	7.2
DK-E	1.3	1.3		0.1		0.2	2.6	2.4	0.4	
DK-W	1.3	1.3		0.1		0.2	3.4	2.0	0.4	
FI	3.1	4.1	0.3	0.2	5.0		2.6	2.6		3.8
IE	0.3	4.6		0.2			3.3	2.5		0.4
NI		1.4		0.1			0.7	0.7		
NL	2.5	17.8	3.5	0.9		0.3	9.2	6.6	6.1	
NO1							0.0	0.0		6.9
NO2						0.4	0.4	0.4		14.2
NO3				0.1			0.3	0.3		4.4
NO4							0.2	0.2		6.0
NO5							0.2	0.2		8.0
SE1							0.9	1.2		4.0
SE2							0.9	1.5		9.5
SE3	3.4	2.3		0.1	9.0		1.9	1.8		2.9
SE4		2.3		0.1			2.8	3.1		1.5
UK-N	0.9	1.1	0.1	0.0	1.4		9.2	7.1	1.8	0.7
UK-M	17.1	20.7	0.3	1.1	6.4	0.8	8.2	6.4		1.1
UK-S		25.3		1.2	9.6		6.6	5.1	9.3	
Sum	37.6	138.8	28.3	6.7	31.3	9.8	120.4	77.6	110.6	70.7

4.3 Production and load data

4.3.1 Load and variable renewable energy production profiles

To realistically model a functioning European power system, hourly load profiles and production profiles for renewable energies are employed for each system node. This allows the model to account for the variability of intermittent renewable energy sources, providing realistic operation of these assets, and helps to distinguish climatic factors such as wind speeds and solar radiation for geographical areas. The load and production profiles are sourced from [40].

Moreover, all load profiles and production profiles for renewable sources stem from the same meteorological year (2005) to account for the correlation between weather, production and electricity demand. To illustrate, a cold winter will increase the demand for heating, and thus increase electricity demand in countries with large shares of electricity-based heating. At the same time, conditions for electricity generation from, for example, wind power might be relatively weak in the particular climate year, which will impact the energy

mix and flow of electricity. Thus, applying the same year allows for implicit modelling of electricity consumption and meteorological condition correlations.

Uncertainty is associated with employing load profiles from a given historical year when modelling a system operating decades ahead. Relatively higher proportions of consumption of electricity, building-mounted generation, local storage facilities, increased adoption of electric vehicles, Smart Grids and smart metering are just a few factors which can influence the demand patterns of the future. Implications on consumption behaviour are also expected when integrating hydrogen as an energy carrier in the European energy system, coupling, for example, transportation and industries to the electricity sector. Future electricity load patterns are, however, outside of the scope of this study but can be an interesting topic to investigate in further works.

4.3.2 Hydropower data

In the model, all existing hydropower plants, reservoir capacities and inflow streams in each bus are aggregated and represented as a single, equivalent plant. Inflows are divided into regulated and unregulated. Models used for the Nordic power systems often emphasis stochastically modelled inflow into hydropower reservoirs [16, 40]. Modelling hydropower at this level would require extensive data gathering, and the substantial increase in complexity will highly impact the running time of the algorithm and is thus considered beyond the scope of this master thesis. This approach to modelling hydropower is also utilised in other studies [17, 45].

Hydropower production and inflow data are provided by [40]. A sample of the input data for hydropower is shown in Table 4.2. As previously seen, most of the hydropower installed is in NO1-5, SE1, SE2, FI and DE, and these areas have the reservoir capacities of significance, with NO2 as the area with by far the largest reservoir capacity. When looking at the regulation factor, most nodes lie around 0.8, expressing a high degree of regulation. With the regulation levels seen, most nodes have substantial ability for regulated production, which should result in a lower production price of hydrogen compared to more rigid production systems, as concluded in the project thesis [7]. Finland has a relatively low regulation factor meaning the FI node has substantially less room for producing hydropower flexibly.

Table 4.2: Hydro power data for selected nodes the 2050 scenario [40]

Area	Reservoir capacity [TWh]	Regulation factor	Regulated production [TWh]	Unregulated production [TWh]
NO2	33.37	0.82	39.30	8.77
NO4	19.62	0.88	19.36	2.66
NO5	13.75	0.84	21.35	3.93
SE1	11.90	0.81	13.70	3.27
SE2	17.36	0.75	29.95	10.00
FI	5.64	0.20	3.28	13.12

Regulated and unregulated inflows are provided in 6-hour mean intervals in the data sets, and are thus linearised to hourly values to fit with the rest of the model. Inflow over the course of the chosen scenario year in NO2 is shown in Figure 4.3 below.

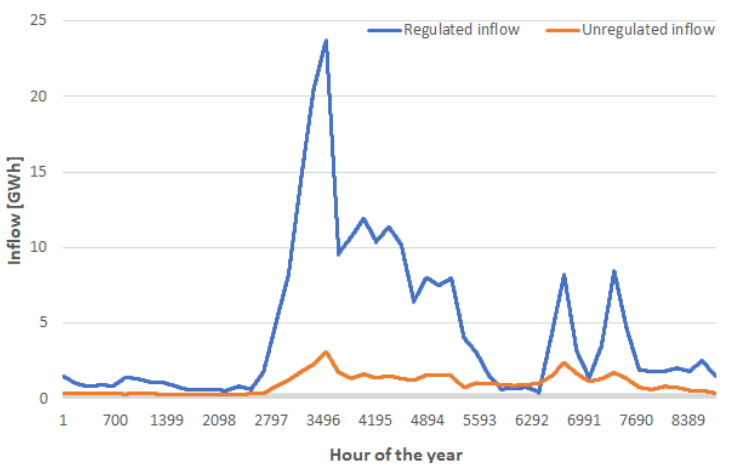

Figure 4.3: Regulated and unregulated inflow in NO2 for the scenario year [40]

As highlighted above, NO2 has considerable volumes of regulated inflow compared to unregulated, which allows for significant degree of control over power generation. A large share of the inflow occurs in the spring and summer months, as a result of snow melting.

4.4 Hydrogen demand

In this study, a hydrogen demand is assumed to be in place in each node in the system, of which the model will try to satisfy in the most cost-effective pathway. The demand is assumed flat on a day-to-day basis. The origin of the demand is not considered but could be expected to influence demand variability as, for example, the seasonality of heating or cooling demands will cause fluctuations in hydrogen consumption in a system where hydrogen is utilised for these purposes.

[46] provides an overview of several studies that have been completed on the use of hydrogen in Europe, with varying degrees of adoption of hydrogen-based technologies. Figure 4.4 shows that hydrogen and synthetic fuels are expected to have a share ranging from less than 1 % to 23 % of the final energy demand in EU. 8 out of 11 studies expect a share equal or larger than 10 %. For these 8 studies, the expected consumption of H_2 and synfuels range from approximately 700 to 2300 TWh in 2050, highlighting a large spread in expectations. The consensus among the scenarios is that the transportation sector will have the greatest demand for hydrogen in 2050, as the majority expects hydrogen and other synthetic fuels to serve 20 to 50% of the total energy demand in transportation.

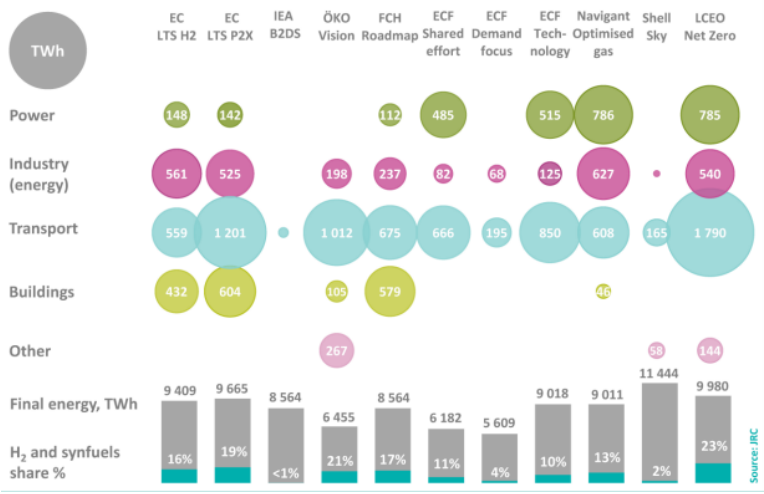

Figure 4.4: Consumption of hydrogen and share in final energy in EU decarbonisation scenarios in 2050 [46]

The hydrogen demand in the base case scenario is set to 8.5 % of the final energy demand in each node. It is set slightly below the shares depicted in Figure 4.4, as these shares also account for other synfuels. Thus, demand for hydrogen is assumed to vary with the final energy demand in each node. The final energy demand for each country in 2050, given in TWh, is sourced from [42], and distributed among the system nodes on the basis of research conducted in [40]. For use in the optimisation model, the energy demand is calculated from TWh to kg using the lower heating value of hydrogen, 33.33 kWh per kg hydrogen [47]. The final energy consumption and hydrogen demand, and the hydrogen demand in tonnes per day are depicted in Figure 4.5 and Figure 4.6. The numerical values are found in Table A.1.

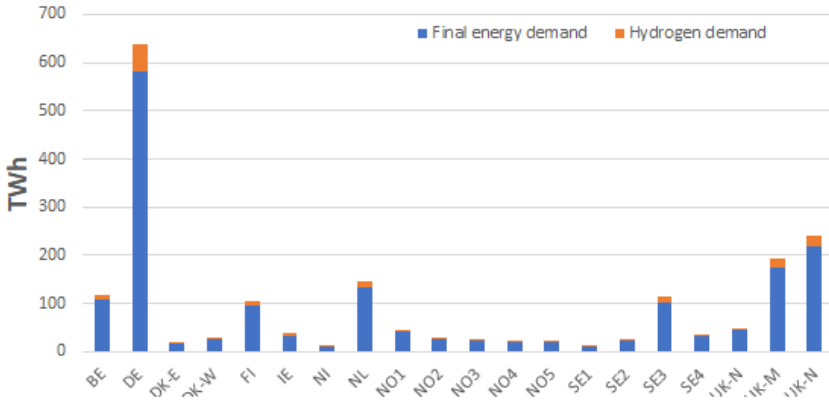

Figure 4.5: Estimated final energy and hydrogen demand in 2050 for each bus

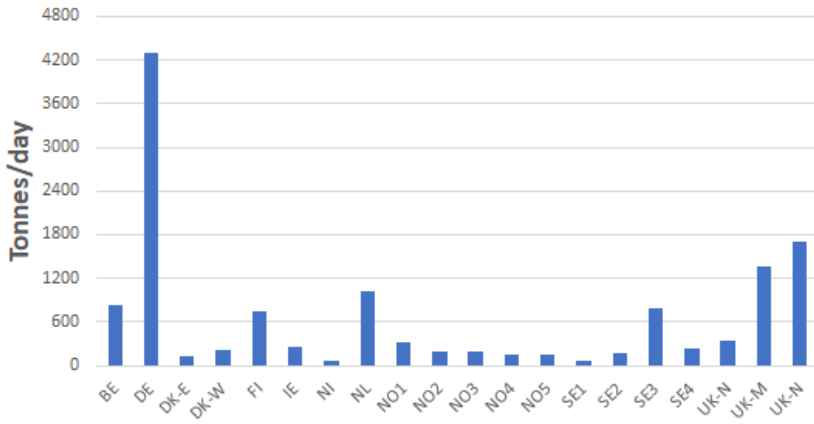

Figure 4.6: Hydrogen demand per day for each bus

4.5 Techno-economic assumptions

The following sections will summarise the applied assumptions regarding the techno-economic parameters of power generation, hydrogen production and storage technologies. The parameters have a critical impact on the modelling results; all of them influence the LCOE, which is calculated implicitly by the model.

4.5.1 Power generation technology costs

NREL's "Annual Technology Baseline provides the techno-economic data used in the model". NREL annually documents a realistic and timely set of technology development assumptions and a wide range of potential futures to inform electric sector analysis in the US. The baseline provides an assessment of current and projected technology cost and performance for both renewable and conventional electricity generation technologies [48].

The model uses annualised costs to calculate the LCOE of each technology endogenously. Equation A.2 is thus used to annualise investment, fixed and variable O&M costs. The resulting annualised technology costs, start-up costs and asset lifetimes are given in Table 4.3. The currency exchange rate used to convert costs from USD to EUR is set to 0.909 EUR/USD [49], and the discount rate is assumed at 6.2%.

Table 4.3: Annualised technology costs, start up costs and lifetime in 2050 [48]

Type	Inv.costs [€/MW-year]	Fixed costs [€/MW-year]	Variable O&M [€/MWh]	Start up costs [€/MW]	Lifetime [years]
Onshore Wind	68209	30000	0.0	0	30
Solar	46082	7273	0.0	0	30
CT Gas	46800	10909	6.4	19	55
CC Gas	46800	10000	2.7	35	55
CCS Gas	100973	30909	6.4	35	55
Coal	207382	30000	4.5	29	75
CCS Coal	298400	72727	9.1	29	75
Nuclear	320364	91818	2.1	97	60
Biomass	210836	101818	5.1	0	45
Offshore Wind	111109	30909	0.0	0	30

The input fuel costs, CO_2 price and energy coefficients in 2050 used in this thesis, are sourced from [40, 48, 50], and summarised in Table 4.4.

Table 4.4: Fuel prices, CO_2 price and energy coefficients [40, 48, 50]

Type	Fuel costs	Unit	Energy coefficients	Ec. unit
CC Gas	11.5	€/MMBtu	0.159	MWh /MMBtu
CT Gas	11.5	€/MMBtu	0.110	MWh /MMBtu
CCS Gas	11.5	€/MMBtu	0.133	MWh /MMBtu
Coal	72.1	€/tonne	7.90	MWh/t
Biomass	2.78	€/MMBtu	0.074	MWh /MMBtu
Nuclear	37.56	€/pound	22.68	MWh/pound
CO_2 price	60	€/tonne		

Other relevant input parameters used in the capacity expansion model are shown in Table A.2 in the Appendix. It must be stated that long-term future technological developments and fuel costs are highly uncertain, as there are many influential factors to future technology and cost parameters. A rise in the costs of raw materials can offset the advances of technological learning and lead to a net increase in specific costs per MW. Consequently, all approaches to forecasting future parameters of generation technologies come with substantial error margin.

4.5.2 Hydrogen production and energy storage assumptions

The PEM electrolyser is chosen as electrolyser technology. The choice is made on the basis of, as mentioned in Chapter 2, significant expected reductions in technology costs, and its favourable characteristics in combination with VRE.

The total future investment costs and fixed costs of the PEM electrolyser amount to 18696

€/(kg/h) and 1311 €/(kg/h) [51], which are annualised over the course of the electrolyser lifetime with a discount rate of 8.3%. The main input parameters for PEM electrolysis is shown in Table 4.5.

Table 4.5: Main input parameters for PEM electrolysis in 2050 [51]

Inv. costs	€/(kg/h)-yr	1568
Fixed costs	€/(kg/h)-yr	110
Variable costs	€/kg	0
Fuel efficiency	kWh/kg	51.3
Size	kg H_2/h	2080
Emissions	kg CO_2/kg H_2	0
Lifetime	years	40
Ramp rate	%/h	1

Two different storage technologies have been identified as relevant, and is thus explicitly included in the model. Lithium ion batteries are utilised as the mean to store electric energy, while hydrogen can be stored in pressurised tanks. The techno-economic assumptions for battery and hydrogen storage are sourced from [48] and [51] respectively. Neither technology have associated variable costs.

Table 4.6: Main battery and hydrogen storage parameters in 2050 [48, 51]

Type	Unit	Inv.costs [€/unit-yr]	Fixed costs [€/unit-yr]	Eff. In/out [%]	Ramp rate [%/h]	Lifetime [years]
Battery power	MW	16491	6205	95 %	100 %	15
Battery energy	MWh	4918	1909			
Hydrogen storage	kg	27	2	100 %	100 %	40

4.6 Hydrogen import from natural gas

Each node has the possibility of importing hydrogen produced from natural gas to serve its hydrogen demand. However, this thesis assumes that only a few nodes will have the capabilities of producing hydrogen from SMR with and without CCS. These nodes have the option to supply their hydrogen demand at a price equal to the SMR production cost, or export to other nodes at the production price plus transportation costs.

4.6.1 Exporting nodes

Most SMR plants today are located near the North Sea, as easy access to natural gas and gas infrastructure is beneficial for low-cost production of grey hydrogen [13]. The Netherlands and the UK are the two leading gas producers in the EU, having a share of more than 60% of the total natural gas production in the EU in 2018. In the same year, Norway supplied 30.2% of the natural gas imported to the EU [52].

An essential factor to consider for future large-scale production of specifically blue hydrogen, and power production with CCS for that matter, is access to CO_2 transportation infrastructure and storage. A promising option is storing sequestered CO_2 in saline aquifers, which are porous and permeable rock reservoirs containing saline fluids, for example, depleted oil and gas fields [53, 54, 55]. The Sleipner CO_2 injection project, located in the North Sea outside of NO5, was the first of its kind and has been both a technical and economic success [56]. As the leading oil and gas producing nations in Europe, Norway, the Netherlands and the UK have significant potential for CO_2 sequestration and storage when considering the possibility of utilising existing gas infrastructure and depleted oil and gas fields.

Consequently, the UK, the Netherlands and Norway are chosen to serve as hubs for centralised hydrogen production from natural gas in the system in 2050. As the UK and Norway consist of multiple nodes, UK-N and NO5 are chosen as the SMR nodes, due to possessing substantial shares of the natural gas production in their respective countries today.

4.6.2 Hydrogen production costs from SMR

To calculate the future production costs of H_2 from SMR, a model for large-scale centralised production, with and without CCS, developed by NREL, is utilised. The main input factors, summarised in Table 4.7, are also provided by NREL [57, 58]. The plant output rate of 500 tonnes/day is insufficient to supply larger hydrogen demand nodes entirely. Thus, it is assumed that the SMR exporting nodes have access to multiple production plants of this scale, with production at the calculated price. The input fuel price corresponds to the price of natural gas utilised in power production described in Section 4.5, equalling a price of 11.4 €/MMBtu [50].

Table 4.7: Main input factors for H_2 from SMR and SMR + CCS cost calculations [50, 57, 58]

Input factors	SMR	SMR + CCS
Fuel price [€/MMBtu]	11.4	11.4
Fuel usage [MMBtu /kg H_2]	0.156	0.156
Operating capacity factor	90.00 %	90.00 %
Plant output [kg/day]	500000	500000
Carbon Capture Efficiency	0.00 %	90.00 %
CO_2 emissions [kg CO_2/kg H_2]	9.27	0.93

The resulting production costs and cost distribution for SMR and SMR + CCS are shown in Table 4.8 and 4.9.

Table 4.8: Total production costs and cost distribution of H_2 produced from SMR

Cost Component	Cost Contribution [€/kg]	Percentage of H2 Cost
Capital Costs	0.13	6.1 %
Fixed O&M	0.05	2.6 %
Feedstock Costs	1.82	87.0 %
Other Raw Material Costs	0.00	0.0 %
Other Variable Costs	0.09	4.3 %
Total	2.09	100.0 %

Table 4.9: Total production costs and cost distribution of H_2 produced from SMR with CCS

Cost Component	Cost Contribution [€/kg]	Percentage of H2 Cost
Capital Costs	0.31	12.9 %
Fixed O&M	0.08	3.4 %
Feedstock Costs	1.82	76.0 %
Other Raw Material Costs	0.00	0.0 %
Other Variable Costs	0.18	7.6 %
Total	2.39	100.0 %

The resulting nodal prices for hydrogen produced from SMR and SMR + CCS in 2050, calculated to 2015 prices, are 2.09 € and 2.39 € respectively. Adding CCS to the production plant increases capital costs, fixed costs and other variable costs by 50-140 %, The nodal prices are the prices given in NI, UK-N and NO5.

4.6.3 Hydrogen transportation

To find the nodal prices in the non-producing nodes, the cost of transporting hydrogen is calculated. Pipelines are used commercially today for large flows of hydrogen and are generally regarded as the most cost-effective transport option [5], and is thus utilised as the mean of transportation in this thesis. The cost of hydrogen pipeline delivery depends on multiple factors, such as capital cost of the pipeline, transport distance and hydrogen flow rate [59]. Comparable to this study, [60] investigates large-scale, and long-distance pipeline transport of hydrogen between Africa and Europe in 2050, and calculations are based on this resource. The main input factors are summarised in Table 4.10.

For simplicity, it is assumed that an import node is supplied from the closest SMR node, and that transmission must occur on land. Thus, NO2 is assumed to supply nodes in Sweden, Finland and the remaining nodes in Norway, UK-N is supplying the rest of Great Britain and Ireland, and NL is supplying Denmark, Germany and Belgium. Transportation

Table 4.10: Input factors for calculating levelised cost of transporting H_2 [60]

Pipeline diameter	inch	48
Number of pipelines		1
Pipeline capacity	GW	10
Specific investment cost	€/10GW/km	1000000
O&M cost	%/yr	1
WACC	%	7
Lifetime	yr	40
Load factor pipeline	hr/yr	4500

distances are estimated between the import nodes and supplier using [61], and the distance is measured as the shortest path, adding an 5 % increase to allow for flexibility.

The pipeline capacity is assumed at 10 GW, which theoretically implies a possible flow of 3 million kg/day, using the stated load factor. This flow is substantial when compared to daily hydrogen demand for some nodes, but opens up for increasing hydrogen consumption and supplying consumption entirely from SMR. Equation A.2 determines the CRF, which is used to calculate the annual investment costs (AIC) of the hydrogen pipelines using Equation A.3. These values are subsequently used in Equation A.4 to calculate the levelised cost of transport (LCOT) for each node. The resulting transport distances, LCOT and total import costs of H_2, produced from SMR and SMR with CCS, for each node are summarised in Table 4.11.

Table 4.11: Transportation distance, transportation costs and total import costs of H_2 from SMR w, w/o CCS for each node

Node	Distance [km]	Transportation costs [€/kg]	Import cost H_2 SMR + CCS [€/kg]	Import cost H_2 SMR [€/kg]
NL	0	0.00	2.48	2.09
DE	380	0.03	2.51	2.12
DK-E	790	0.06	2.54	2.15
DK-W	860	0.06	2.54	2.15
BE	160	0.01	2.49	2.10
NO2	0	0.00	2.48	2.09
FI	1400	0.10	2.58	2.19
NO1	360	0.03	2.51	2.12
NO3	620	0.05	2.53	2.14
NO4	1500	0.11	2.59	2.20
NO5	300	0.02	2.50	2.11
SE1	1300	0.10	2.58	2.19
SE2	840	0.06	2.54	2.15
SE3	525	0.04	2.52	2.13
SE4	890	0.07	2.55	2.16
UK-N	0	0.00	2.48	2.09
IE	630	0.05	2.53	2.14
NI	470	0.03	2.51	2.12
UK-M	470	0.03	2.51	2.12
UK-S	810	0.06	2.54	2.15

4.7 Transmission

In the system investigated in this master's thesis, each node has the option for exchanging power with the electricity grid. As previously discussed, transmission between system nodes is only restricted by the capacity of the transmission lines. Moreover, the expansion of new energy generation by the investment algorithm is assumed to occur in close proximity to current production assets. Existing electricity grid, assumed to have sufficient capacity, is thus utilised for transportation from production to the load centres. National distribution grids are not modelled, except for countries represented by multiple nodes.

Future transmission connections and line capacities estimates were provided by Steve Völler [40]. The transmission system utilised is depicted in Figure 4.7, showing the interconnections between nodes with their respective transmission capacities. Numeric values are listed in Table A.3 in the Appendix.

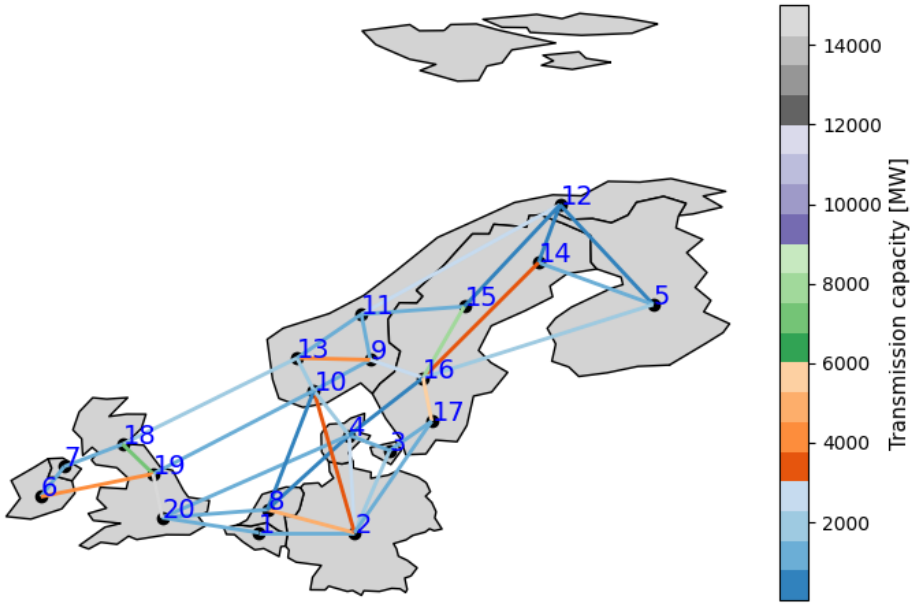

Figure 4.7: Interconnections and capacities between the system nodes in 2050

For simplicity, the nodes are assumed not to interact with areas outside the system. Although this assumption is not entirely realistic due to the interconnectivity of the European power system, it allows for investigation of effects of hydrogen integration without interference from power exchange with outside areas. Several previous studies involving a European power system have used this assumption to define the system boundaries [62, 63].

Chapter 5

Results

The subsequent chapter presents the results from the capacity expansion model in the following structure.

- Base case scenario
- The base case run for no initial capacity installations, and variations in VRE and electrolyser CAPEX, and hydrogen demand
- Sensitivity analysis on the price of CO_2
- Sensitivity analysis on the cost of natural gas at different CO_2 prices

Due to the vast quantity of results, the results are briefly commented in this section, before they are subject to more thorough reflection in the discussion in Chapter 6.

5.1 System development in 2050 base scenario

5.1.1 Capacity expansion

Figure 5.1 depicts the capacity investments for each node in the base case scenario. Installed capacities in hydrogen electrolysers and batteries are also included for each bus.

The results show that the investments in new capacity mainly occurs in onshore and offshore wind, with wind power investments in the 10-55 GW range. Most nodes also invest in electrolyser capacity, which amount to approximately 40 GW for the system in total.

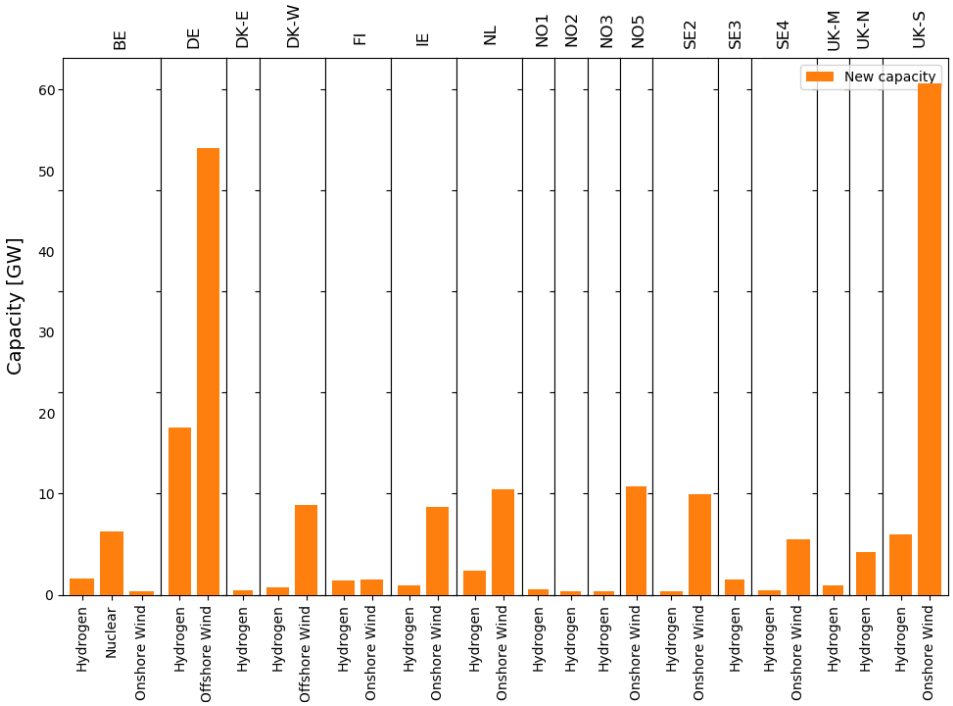

Figure 5.1: New capacity (bigger than or equal to 0.3 GW) by bus and technology for the base case

The production output capacities from electrolysis, as a result of electrolyser investments, are depicted in Figure 5.2.

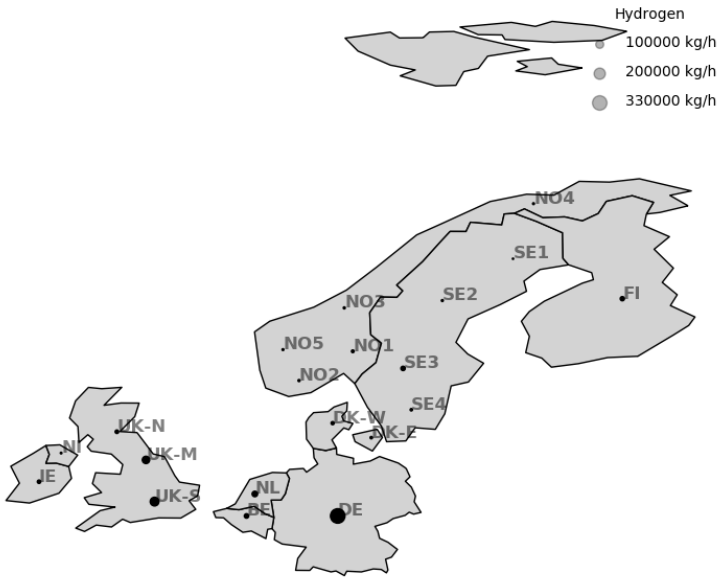

Figure 5.2: Hydrogen production capacity in each node

DE has the greatest output capabilities of the nodes, amounting to 330000 kg H_2 per hour from electrolysis. The UKs have capabilities of about 200000 kg/h, while smaller demand nodes like the Nordics require capacities slightly below 100000 kg/h.

5.1.2 Power generation mix

Figure 5.3 depicts the electricity generation mix for the base case scenario.

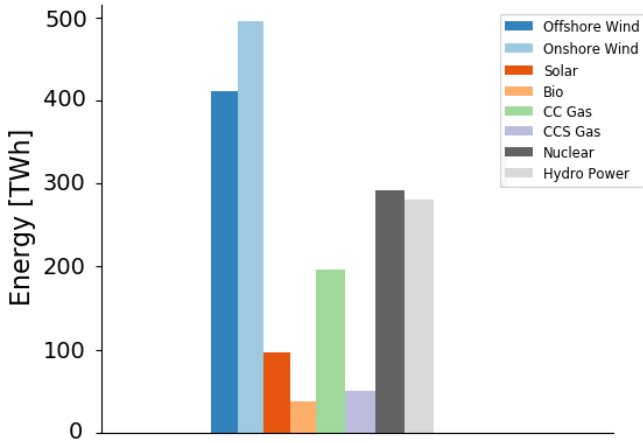

Figure 5.3: Amount of energy generated by type by the system in 2050

Onshore and offshore wind are the main electricity contributors. Nuclear, hydropower and CC gas also supply a substantial share of energy.

The electricity generation mix for the system for the first ten days of March in 2050 is depicted by Figure 5.4. The figure shows how electricity production in the system fluctuate, especially from VREs.

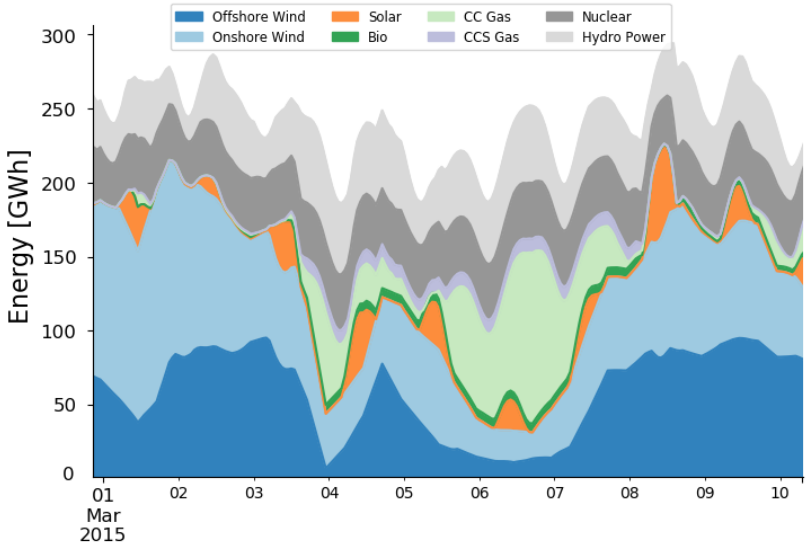

Figure 5.4: Electricity generation mix for the system in the first ten days of March

Imports and exports of electricity for each node in the base case scenario in shown in Figure 5.5.

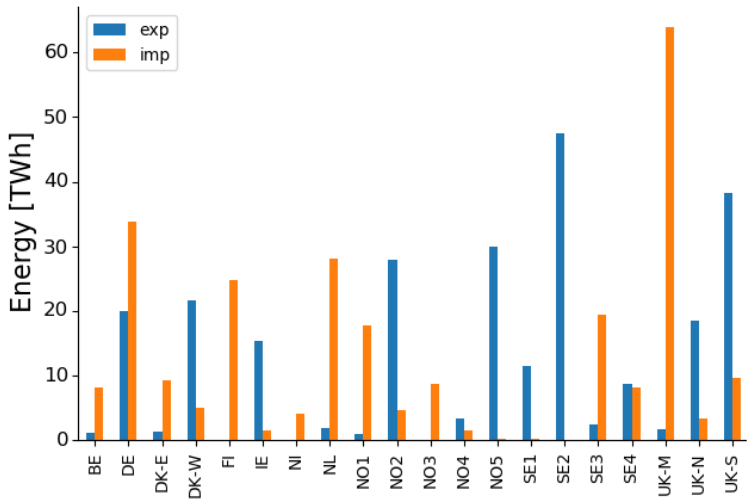

Figure 5.5: Energy import and export by bus

5.1.3 Large scale hydrogen production

The distribution between the different origins for hydrogen in the system is given in Figure 5.6.

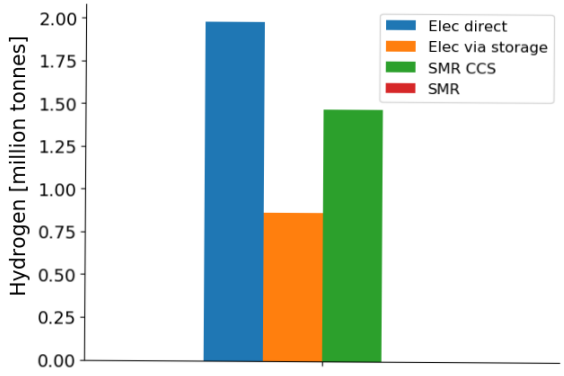

Figure 5.6: Hydrogen distribution by source in the base case

The figure shows a gravitation towards electrolysis-based H_2, as the greater share of production stems from electrolysis supplying hydrogen directly to the hydrogen load or via storage before consumption.

Furthermore, the distribution of the source of hydrogen vary between the system nodes, as depicted by Figure 5.7.

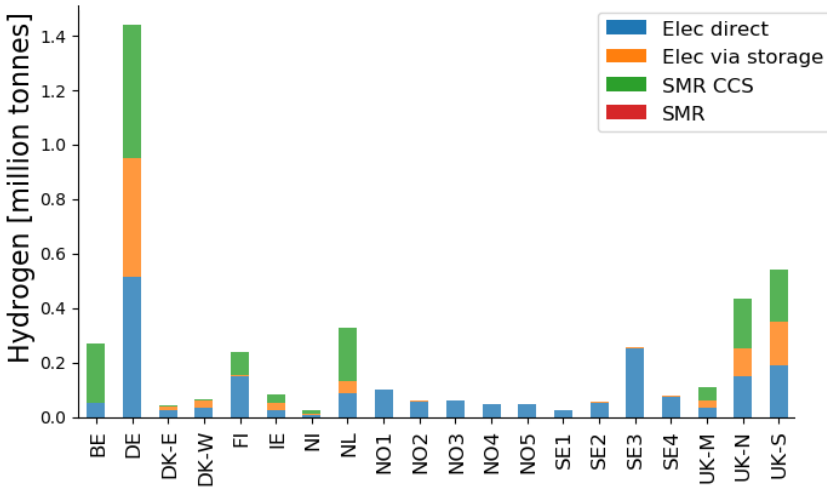

Figure 5.7: Hydrogen distribution by source for each node in the base case

The results indicate that most nodes mainly favour hydrogen produced from electrolysis. However, most nodes import hydrogen from natural gas with CCS to supply a significant share of their hydrogen consumption, except for the NOs and SEs, where electrolysis constitute the entire hydrogen production.

The average marginal cost of production per kg hydrogen in each node is depicted in Figure 5.8. The prices are calculated from the hydrogen price, using the dual variable of the hydrogen balance in Equation 3.9, and accounting for each node's production distribution and the aggregated system production.

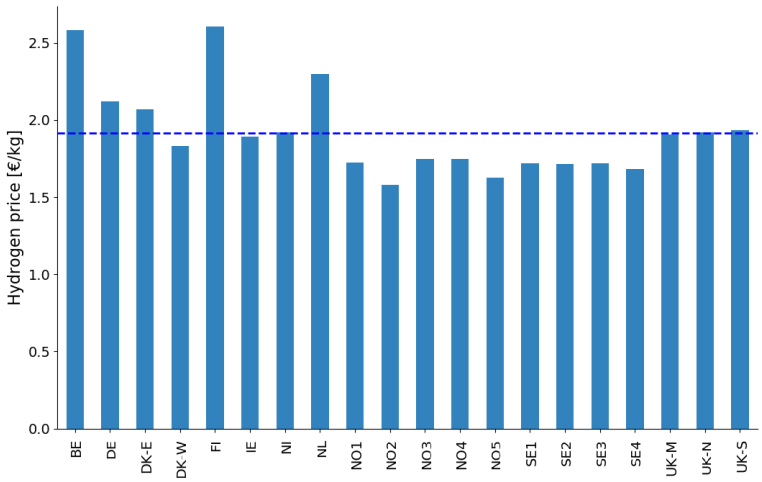

Figure 5.8: Cost of hydrogen production for each node and average price

5.1.4 Storage investments and utilisation

Investments in hydrogen storage facilities and storage capacity in kg are shown in Figure 5.9.

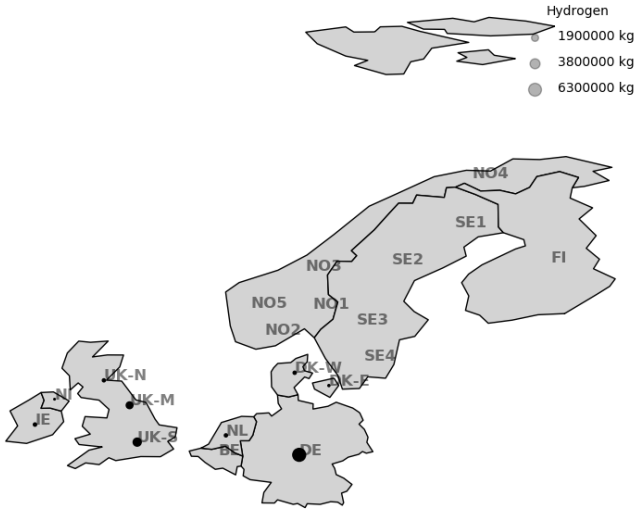

Figure 5.9: Hydrogen energy storage installed in each node

Storage capacities in DE are sized at 160 % of daily demand, while the UK nodes have storage compared to daily demand in the 250-625 % range, covering several days. On the contrary, almost no storage capabilities are introduced in the nodes in the Nordics, excluding DK-E and DK-W.

The resulting storage utilisation for nodes with installed storage options for the first ten days of March is shown in Figure 5.10.

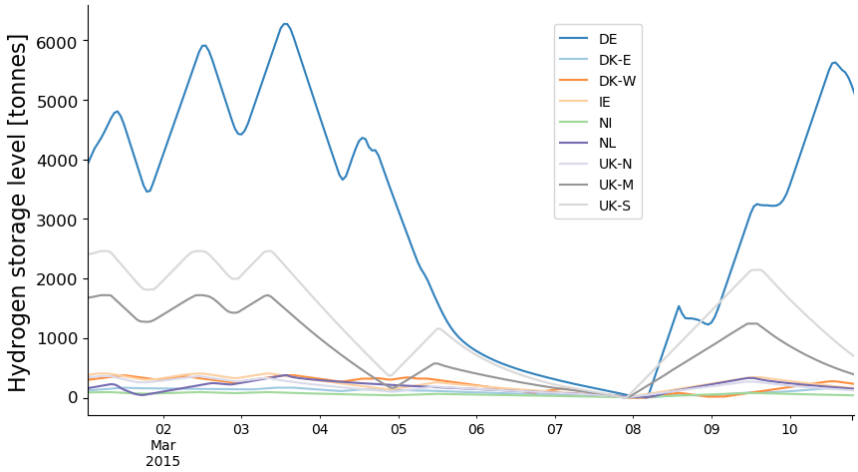

Figure 5.10: Hydrogen energy storage level for each bus in March

5.2 Base case variations

This section will present results of effectuating the model for different variations of the base case scenario.

5.2.1 Designing the optimal generation mix

To investigate the optimal capacity expansion and the mix of generation technologies for the system without the expected installations from designing the scenario, the capacity expansion model is run with no initial power generation capacities installed. Due to the geographical restrictions of hydropower, hydropower capacities are set to the base case levels. The resulting investments in generation capacities, electrolysers and storage for each node are depicted in Figure 5.11

Investments in battery capacity are observed in some nodes, varying between 600 and 2100 MW, as shown in more detail in Figure 5.12.

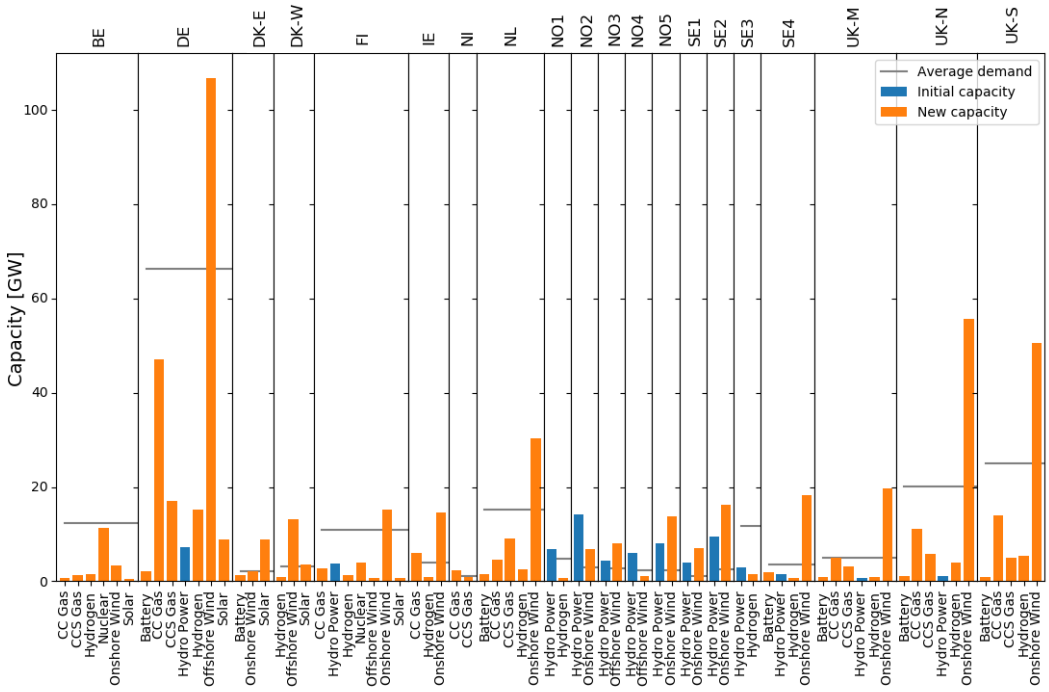

Figure 5.11: Expansions in capacity (bigger than or equal to 0.4 GW) by bus and technology without initially installed capacities

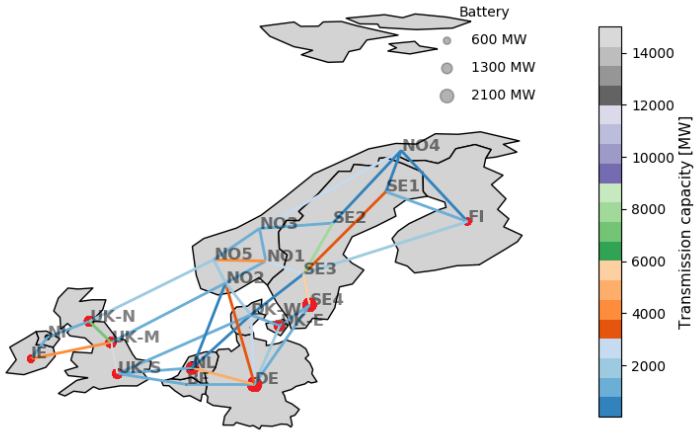

Figure 5.12: Battery capacity installation and transmission capacities in the optimal simulation

The resulting energy mix, shown in Figure 5.13, constitutes of large shares of electricity coming from both wind assets, in addition to significant shares from CC gas, CCS gas and hydropower.

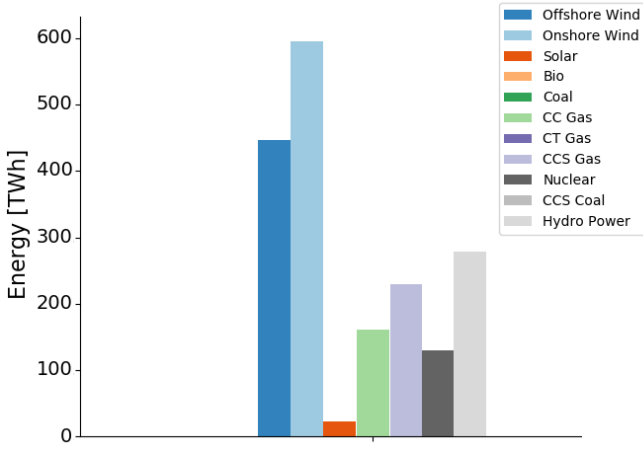

Figure 5.13: Electric energy generation by type with optimal capacity investments

5.2.2 Effect of variable renewable energy and electrolyser CAPEX

To investigate the influence of the estimated future capital costs of wind, solar and electrolyser technologies on the hydrogen production in the system, simulations with a 100 %

increase and a 50 % reduction in capital expenditures are performed.

Sources of hydrogen

Hydrogen production in the system is entirely based on imports from SMR with CCS, as consequence of doubling VRE and electrolyser CAPEX, shown in Figure 5.14.

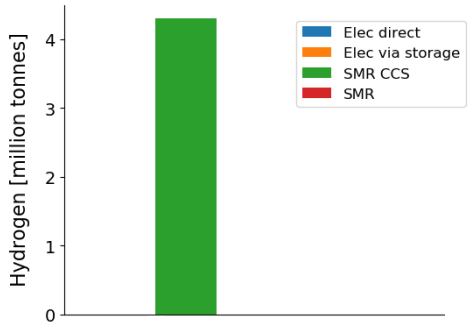

Figure 5.14: Hydrogen distribution by source with a 100 % increase in VRE and electrolyser CAPEX

On the contrary, when the capital expenditures are halved, Figure 5.15 show that SMR with CCS only constitute about 10% of the hydrogen supply in the system. 40% of the hydrogen produced from electrolysis is sent via storage.

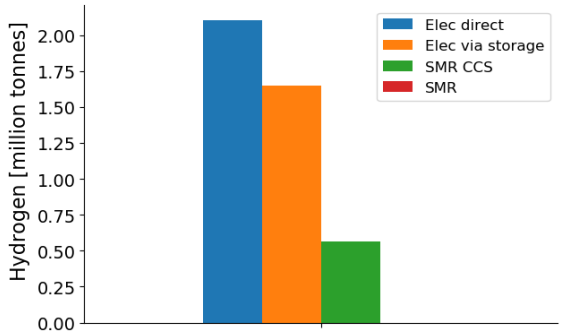

Figure 5.15: Hydrogen distribution by source with a 50% reduction in VRE and electrolyser CAPEX

Cost of hydrogen

The cost of hydrogen production from doubling and halving the capital expenditures are shown in Figure 5.16 and 5.15 respectively.

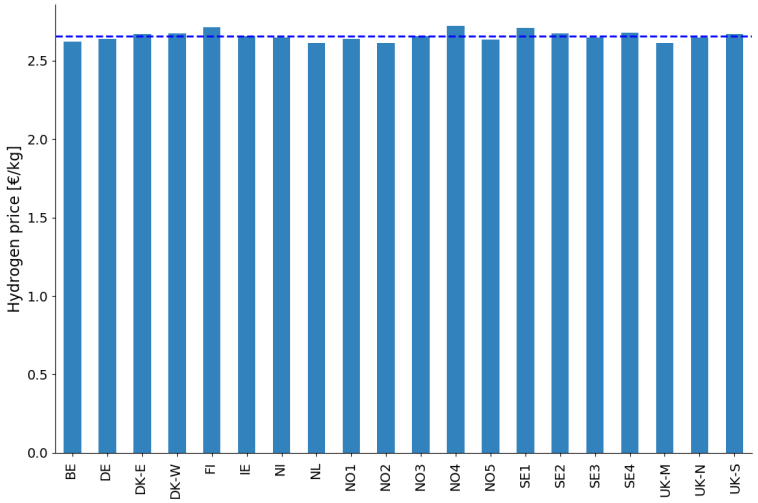

Figure 5.16: Cost of hydrogen for each node with a 100 % increase in VRE and electrolyser CAPEX

The cost of producing hydrogen at elevated CAPEX levels is more or less the same for all nodes, stabilising around 2.6 €/kg H_2. Lower CAPEX levels causes significant variation in the production cost of hydrogen, from 0.85 €/kg in NO2 to 1.96 €/kg in BE.

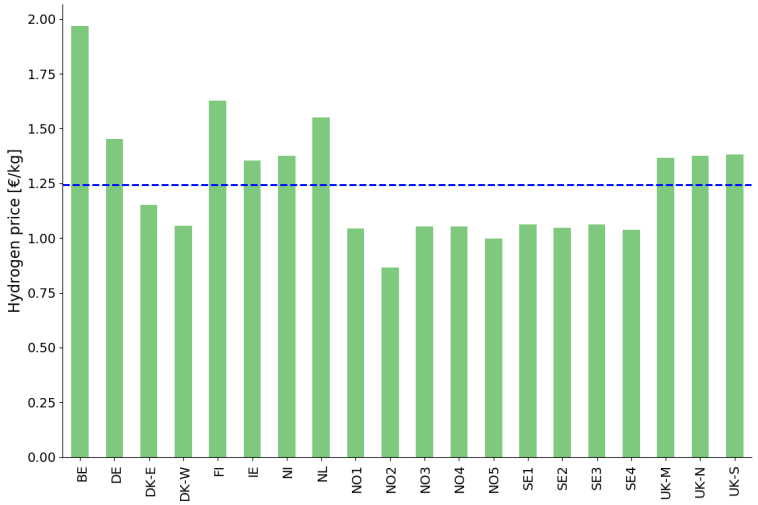

Figure 5.17: Cost of hydrogen for each node with a 50 % reduction in VRE and electrolyser CAPEX

5.2.3 Effect of hydrogen demand

As seen in the scenario building chapter, there are large deviations among studies on the level of expected hydrogen demand in Europe in 2050. To study the effects of hydrogen demand on the future European energy mix, the optimisation model is executed for scenarios with no hydrogen demand, and twice and quintuple the base case value set for each node.

Changes in the energy mix for different levels of hydrogen demand for each node relative to the base case level is shown in Figure 5.18 below.

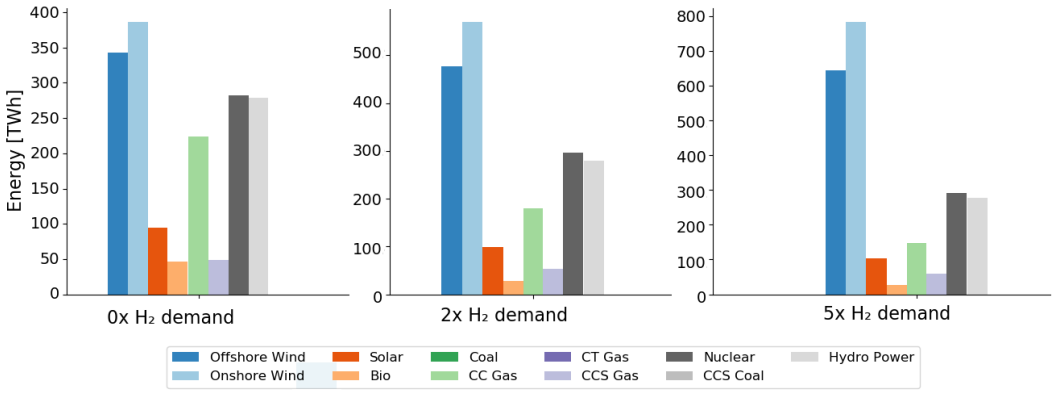

Figure 5.18: Sum of energy by type for zero, two and five times the base case H_2 demand

The system for all levels of demand receives the larger share of electricity from wind power. At no hydrogen demand, CC gas, nuclear and hydropower constitute a large portion of the energy produced. At twice and quintuple demands, the production levels from these energy generation types remain constant, thus lowering their share of the total production.

The hydrogen production source distribution for 5 times the base case hydrogen demand is depicted in Figure 5.19.

The figure shows that the system uses electrolysis to directly supply the hydrogen demand in combination with SMR with CCS. Storage is utilised to a relatively small extent.

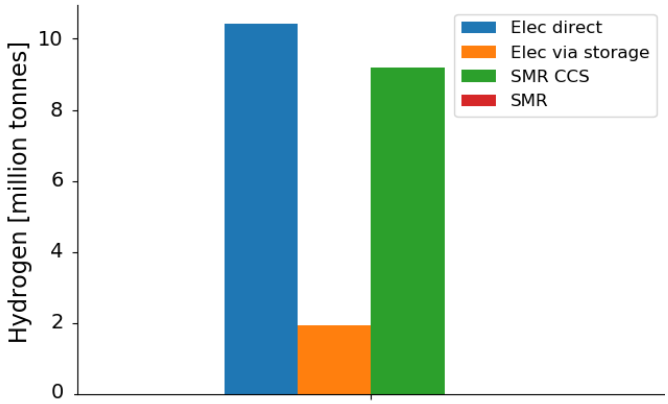

Figure 5.19: Hydrogen production source distribution 5x H2 demand

5.3 Sensitivity analysis of the CO_2 price

Several exogenous model inputs can influence system behaviour. In this section, the effect of the CO_2 price on the model outcomes is investigating with a sensitivity analysis The model is executed for range of 0 to 270 €/tonne CO_2, with increments of 30 €/tonne, to investigate impacts of the CO_2 price on the system.

5.3.1 Energy generation

The energy generation mix for increasing CO_2 prices is depicted in Figure 5.20.

The results indicate that coal, CC gas and CCS gas are the main energy sources affected by deviations in carbon dioxide pricing from the base case level. Offshore and onshore wind production increase with rising CO_2 prices until 90 €/t CO_2.

The sum of energy produced by each asset type for an increasing cost of CO_2 is depicted in Figure 5.21. A reduction in electricity produced from CC gas from 290 TWh to 20 TWh is observed in the chosen price span. Production from CCS rise steadily from zero, reaching peak production at 210 €/t CO_2 of 150 TWh.

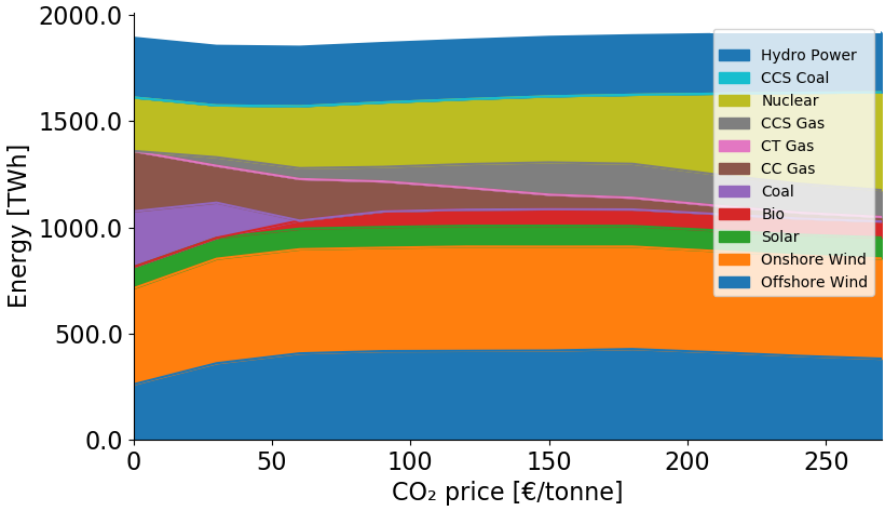

Figure 5.20: Sum of energy by type for increasing CO_2 prices

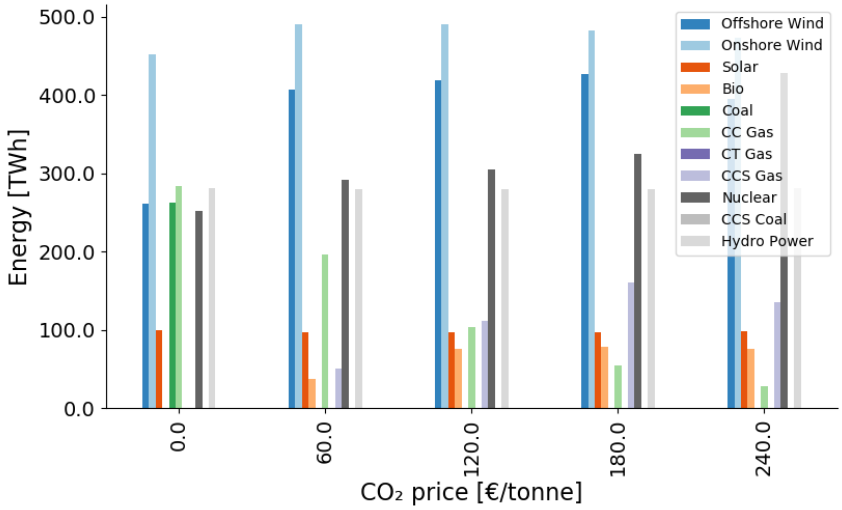

Figure 5.21: Sum of energy by type for increasing CO_2 prices

The price of CO_2 has significant effect on the total emissions of the system, shown in Figure 5.22. The graph includes emissions related to hydrogen production from SMR with and without CCS.

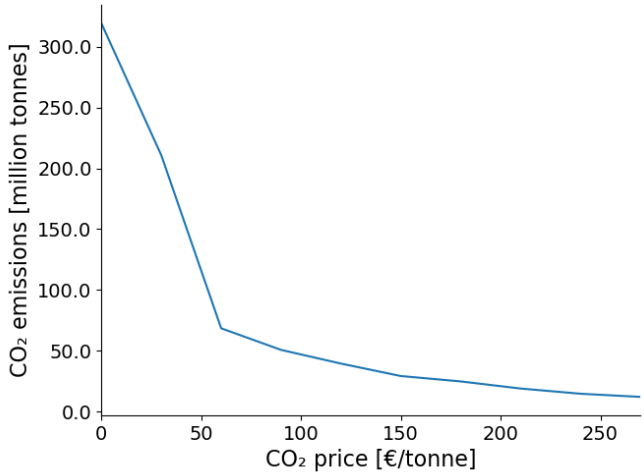

Figure 5.22: Total CO_2 emissions for the system for increasing CO_2 prices

5.3.2 Hydrogen production

CO_2 costs have been observed to be highly impactful on the energy generation mix. Carbon price levels also affect hydrogen production, as given by the distribution of hydrogen production by source for increased prices of CO_2 in Figure 5.23.

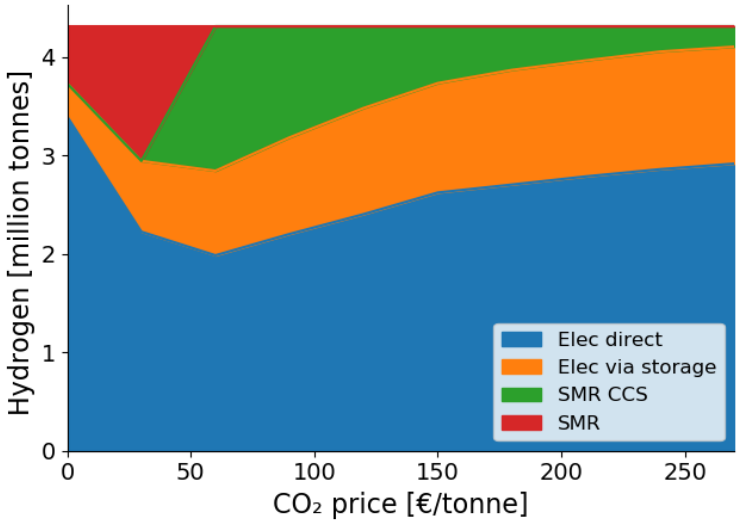

Figure 5.23: The source of hydrogen for increasing CO_2 prices

The results show an initial large production of H_2 from electrolysis, with relatively small amounts channeled via storage, and about 12 % SMR-share. SMR then sees peak share of 32 % of the hydrogen supply. Moving forward from 60 €/tonne CO_2, the share of electrolytic hydrogen increase steadily, both for direct use and stored hydrogen. Simultaneously, hydrogen from SMR with CCS decline with growing carbon costs, as the CCS-technology fails to capture all emissions.

Production price variations for the system nodes as a result of changing CO_2 prices are shown in Figure 5.24.

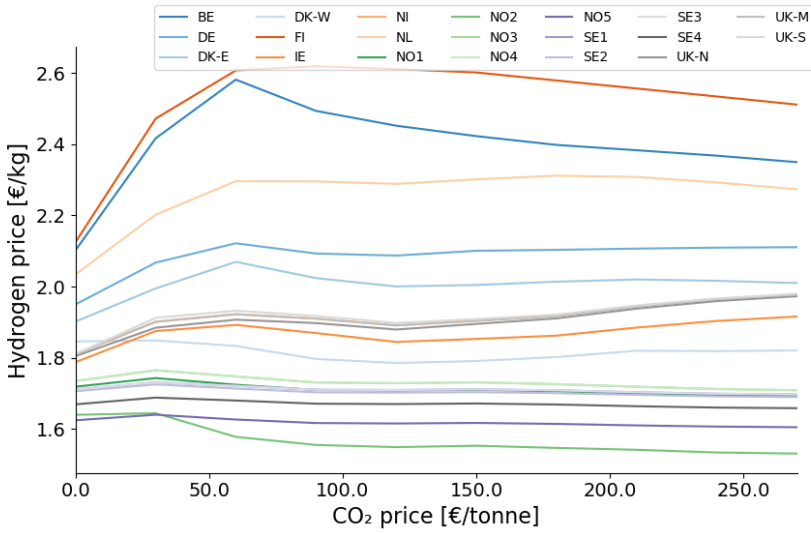

Figure 5.24: Average price of hydrogen in each node for increasing CO_2 prices

Steady prices between 1.6 and 1.75 €/kg H_2 are observed for most nodes located in Norway and Sweden. Nodes in the UK, DE and DK are subject to higher pricing, which increase slightly with rising CO_2 prices in the 1.8 to 2.1 €/kg H_2 range. Costs of hydrogen in BE and FI jumps largely at a carbon dioxide cost of 60 €/t.

The cost of carbon dioxide also influence the average price of electricity seen by electrolysis in each node, as depicted in Figure 5.25.

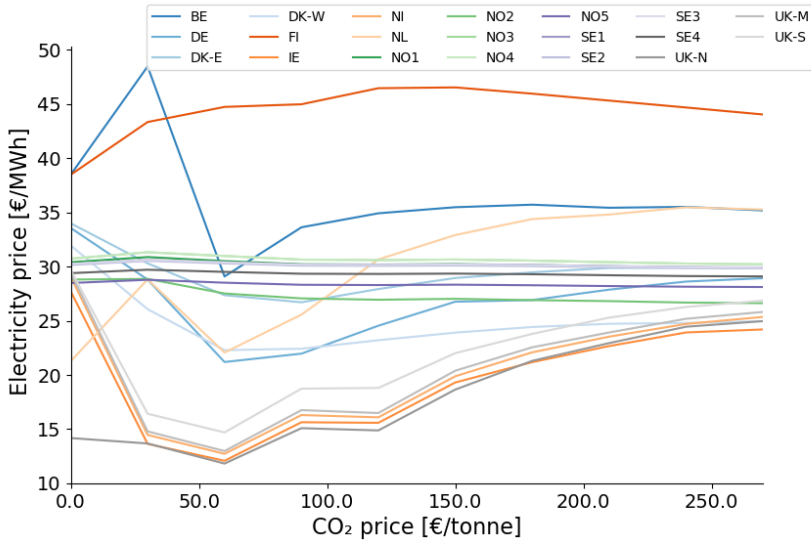

Figure 5.25: Average price of electricity seen by electrolysis in each node for increasing CO_2 prices

The price is calculated from dual variable of the electric energy balance, and describes the market price seen in each node at increasing CO_2 costs. The electricity price remains stable around 30 €/MWh in the NOs and SEs, the nodes supplied mostly from hydropower. The market price in DE, NL and UK experience an initial drop, before gradually increasing with the price of CO_2. Finland is subject to high pricing due to rationing costs.

5.4 Sensitivity analysis of the natural gas price

Natural gas price forecasts towards 2050 are influenced by various factors and subject to notable uncertainty, thus representing significant unreliability in the system. To investigate the effect of the price of natural gas in 2050, the model is effectuated for a range of price levels, at two different CO_2 price levels. The range spans from a 50 % decrease in the base case price level of 39.06 €/MWh to a 50 % increase, with increments of 10 percentage-points. The variation in natural gas price is represented as price scaling relative to the base case price, which is equal to a scaling factor of 1.0.

5.4.1 Energy generation

CO_2 = 60 €/t

The electric energy generation mix for various price levels of natural gas at a CO_2 price of 60 €/t is shown in Figure 5.26. CC and CCS gas produce about 500 TWh of the energy with NG prices halved, before being replaced by biomass, coal and nuclear at higher price levels.

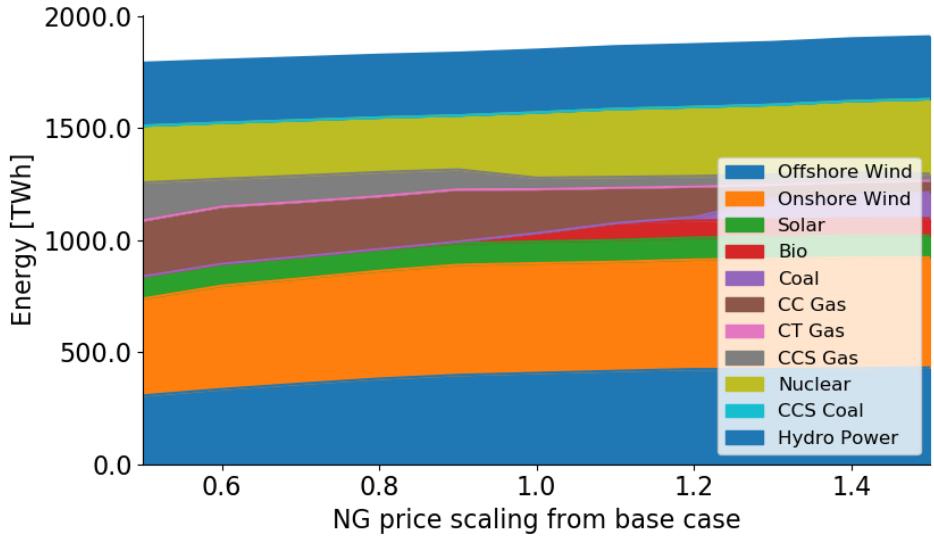

Figure 5.26: Electrical energy production by production type for different prices of natural gas at CO_2 = 60 €/t

CO_2 = 0 €/t

The electric energy generation mix for various price levels of natural gas with no carbon dioxide cost is shown in Figure 5.27.

Combined-cycle gas represents the greatest share of generation at 50 % reduction in natural gas prices. Coal also has a relatively large share, and is the preferred asset investment with the price of CO_2 at 0 €/tonne, in tandem with onshore wind, gradually taking over production from gas at greater price levels as seen from Figure 5.28 below.

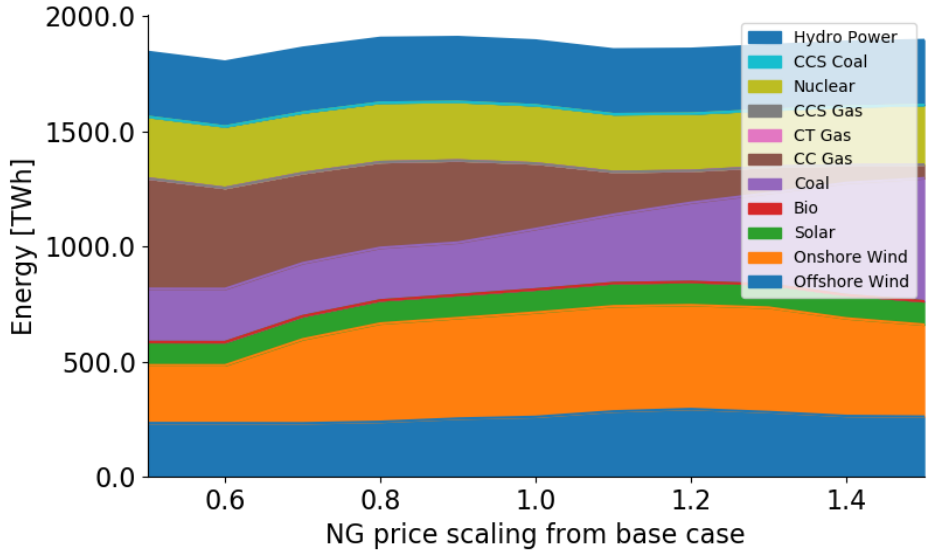

Figure 5.27: Electrical energy production by production type and sum of production for different prices of natural gas at no CO_2 = 0 €/t

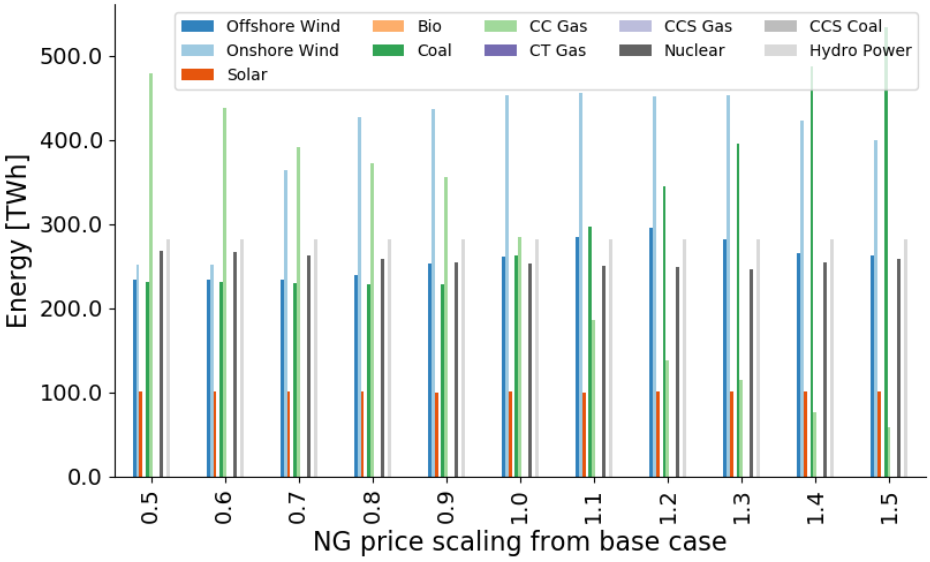

Figure 5.28: Electrical energy production by production type for different prices of natural gas at no CO_2 = 0 €/t

The generation from offshore wind, nuclear, solar and hydro power stays relatively flat for

the entire price span.

At no cost of carbon dioxide, total system emissions vary in great magnitude with the price of natural gas, as depicted in Figure 5.29.

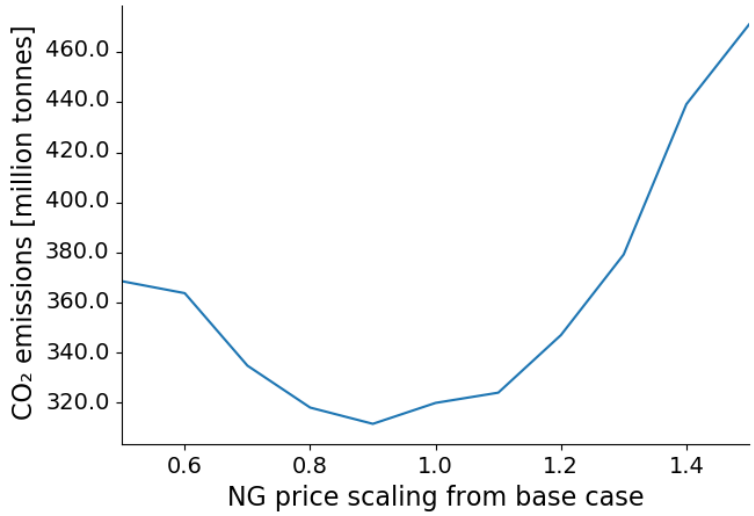

Figure 5.29: CO_2 emissions for different prices of natural gas at no CO_2 = 0 €/t

A 50 % reduction in gas prices results in total system emissions of 370 million tonnes of carbon dioxide. The lowest level of emissions are seen at a price reduction of 10 pp, with emissions levels spiralling more than a 100 million tonnes with increasing prices.

5.4.2 Hydrogen production

CO_2 = 60 €/t

Figure 5.30 and 5.31 depicts the source of hydrogen for increasing gas prices at a CO_2 price of 60 €/t.

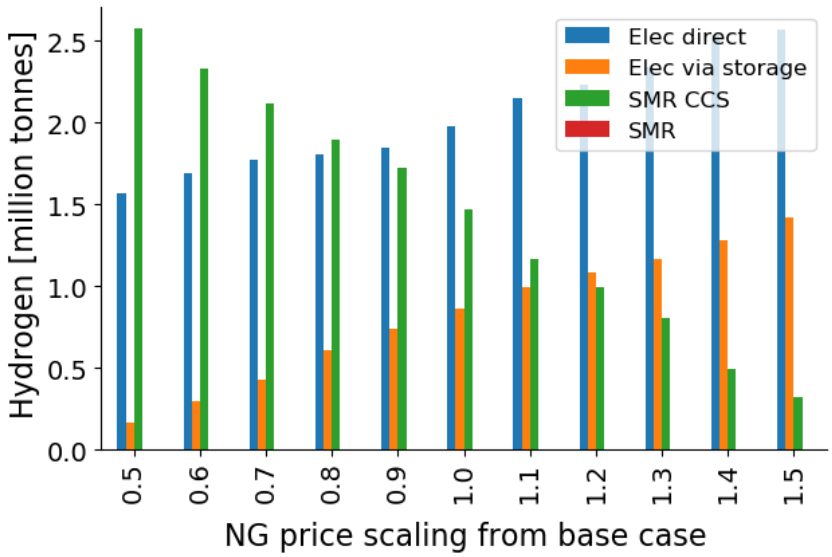

Figure 5.30: The source of hydrogen for increasing gas prices at CO_2 = 60 €/t

Hydrogen produced from SMR with CCS is the favoured production pathway at lower natural gas price levels. Relatively small amounts of hydrogen sent via storage is seen for low gas prices, as import from SMR reduces the need for storage flexibility. A rise in the base case price further increases the electrolysis production share.

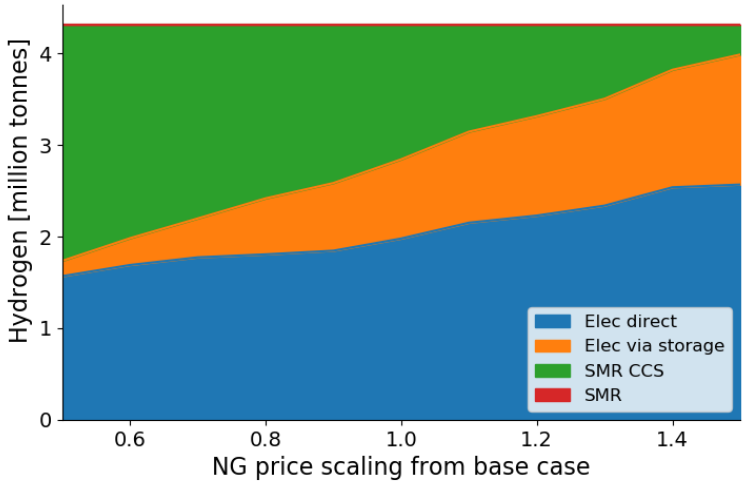

Figure 5.31: The source of hydrogen for increasing gas prices at CO_2 = 60 €/t

As seen from the slope of Figure 5.31, electrolysis via storage has a higher growth rate compared to direct electrolysis for increasing prices of natural gas.

CO_2 = 0 €/t

Figure 5.32 shows the source distribution of hydrogen for various NG prices with no carbon dioxide cost. Electrolysis is observed to have the greater share for most price levels, with varying production from SMR and little storage utilisation.

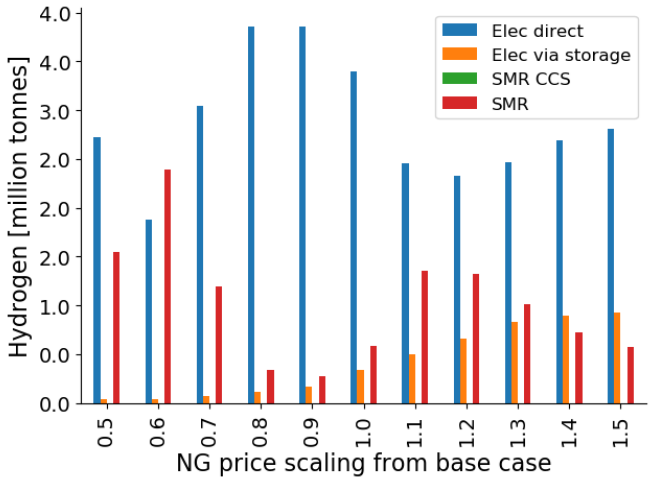

Figure 5.32: The source of hydrogen for increasing gas prices at CO_2 = 0 €/t

The distribution for each node at a 50 % reduction in price is depicted in Figure 5.33.

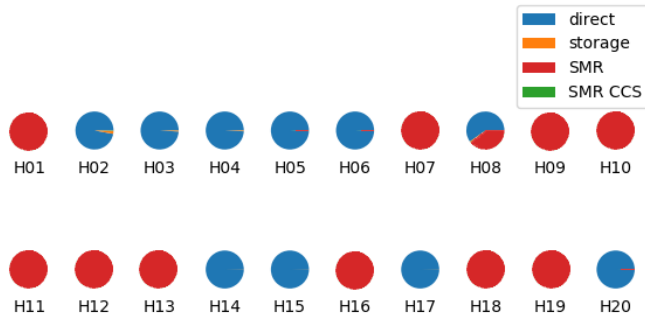

Figure 5.33: Distribution of hydrogen sources for each node for at a 50% reduction in NG pricing and CO_2 = 0 €/t

5.4.3 Hydrogen production costs

The average hydrogen production cost for various natural gas price levels at no CO_2 cost is shown in Figure 5.34. Low prices of natural gas lowers the cost of hydrogen, gradually rising with increasing NG prices.

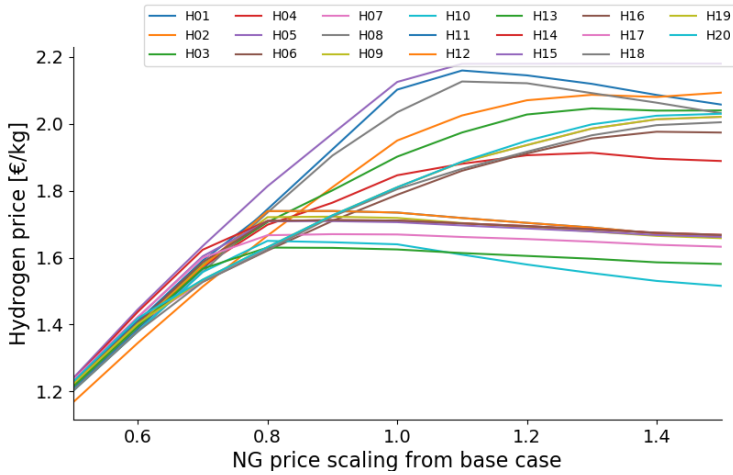

Figure 5.34: Average hydrogen production cost for each node at different NG prices with no carbon dioxide cost

Chapter 6

Discussion

This chapter discusses the results from simulating the 2050 base scenario in terms of capacity expansion, energy generation mix, sources of hydrogen, hydrogen production costs and electrolyser and storage utilisation. Elements from variations of the base case are used for comparison. Implications of the CO_2 and natural gas price on the energy mix, hydrogen production and costs from the marginal analyses are also discussed. Lastly, methodology and scenario shortcomings are discussed.

6.1 Capacity expansion

In the base case scenario, new electricity generation capacities are solely based on low carbon sources, as depicted in Figure 5.1. The development in technology costs and a carbon price of 60 €/tonne lays the ground for a healthy investment climate for large scale expansion of low carbon energy sources. As a consequence, substantial growth in wind generation capacity is observed in several nodes. Around 40 GW of offshore wind is installed in Germany, in addition to about 7 GW in DK-W, while onshore wind is installed at even greater levels and spread over multiple buses. A large share of the onshore wind installed is concentrated in UK-S, with more than 50 GW developed, although NO5, SE2, SE4, NL and IE (and to some extent BE, SE4 and FI) are also subject to heavy expansions in the 10-15 GW range. One can question the viability of expanding wind power of this magnitude in such geographical concentration and proximity to load centres. However, this discussion is outside the scope of this thesis.

Further, solar PV sees no capacity expansion. The cause is most likely that the system under investigation is located in Northern Europe where irradiation conditions are less favourable to, for example, Southern Europe, consequently making wind power relatively better off. This is in line with previous research on a decarbonised European power system

in 2050, based on optimisation modelling, which finds moderate proportions of solar PV installed [30]. Solar PV can also be affected by the input production profiles. A drawback of this study is that production and load profiles are based on a single weather year, while annual variations in output patterns must be expected, meaning that the chosen year can be particularly disadvantageous for solar PV. Simulating the system for a series of weather years to investigate for variations in RES capacity expansion is an interesting task for further works. To summarise, the cost reductions seen by onshore and offshore wind combined with significant expansion potentials and favourable wind conditions elevate wind power as the generation asset of choice.

6.2 Energy generation mix

In terms of energy generation, electricity from onshore and offshore wind amounts to 26.5 and 22.0 % respectively of the total electricity produced in the base case system, as indicated by Figure 5.3. Despite significant initial capacities installed in some nodes, solar PV only supply about 5 % of the electricity. Nuclear power is the dominant non-renewable energy source, with a share of 15.8 %, followed by 10.6 % from CC Gas. In addition to CCS Gas, they make up the entire share of generation from conventional power at approximately 30 %. Hydropower also supplies a substantial share of energy, adding up to 15.1 % of the total supply. Of the total energy produced, the system hence comprises of about 70 % of stemming from renewable sources, and can be characterised as largely penetrated by RES.

Under circumstances of high RES shares, [30] finds that exploiting the full generation potential of the installed capacity at a site is usually not economical. The infrastructure necessary to make use of 100% of the energy produced is expensive due to low utilisation, despite the deployment of energy storage. Consequently, a portion of the electricity generated is curtailed. When considering curtailment of 3.34% of the renewable energy produced in the base case, the system consequently has a net renewable share of 67.06%, calculated from Equation A.1 in the Appendix.

The high renewable share has noteworthy implications for the power system operation. Figure 5.4 provides a snapshot of the electricity generation mix for a week in March for the system as a whole. Hydropower and nuclear is producing steadily throughout the period, providing baseload power in conjunction with both wind asset classes. Electricity is also supplied by solar PV for a few hours during the day. The results highlight the unreliability of RES, a key challenge to large-scale integration and decarbonisation of the electric power system. From day four and onwards, significant fluctuations in wind generation are observed. Energy output fluctuates between 150.000 and 50.000 MWh in a matter of days. Even more extreme, from 150.000 to 50.000 MWh within day three to four. As a consequence, the dispatchable capabilities of CC gas, CCS gas and biomass are used a buffer to serve the remainder of the demand. This underlines the importance of back-up power generation or other dispatchable sources for a system largely penetrated by renewable energy sources.

6.2.1 Comparison between base and optimum

When comparing the original system and the optimal system, where the model is allowed to optimise the power system evolution in 2050 except for hydropower installations (Figure 5.11 and Figure 5.13), some deviations in the energy mix are observed , as summarised in Table 6.1.

Table 6.1: Energy generation mix, curtailment and net RES share for the base- and zero case

	Base case	Optimum
Offshore Wind	22.00 %	23.97 %
Onshore Wind	26.50 %	31.97 %
Solar	5.20 %	1.23 %
Bio	2.10 %	0.00 %
Coal	0.00 %	0.00 %
CC Gas	10.60 %	8.60 %
CT Gas	0.00 %	0.00 %
CCS Gas	2.80 %	12.34 %
Nuclear	15.80 %	6.95 %
Hydro Power	15.10 %	14.94 %
Curtailment	3.34 %	3.90 %
Net RES share	70.90 %	72.11 %

The optimal case exchanges baseload generation from nuclear with a substantial increase in production flexibility from CCS gas, allowing more onshore and offshore wind to penetrate the system, consequently increasing the net renewable share slightly, with a small increase in curtailment. RES-integration is also helped by battery installations, occurring in most nodes without significant access to hydropower, seen from Figure 5.12. Although battery usage only add up to 0.67 % of the total energy produced. The results seen for solar PV are in line with the previous discussion, considering that solar constitutes only 1.23 % of the generation mix in the optimum case.

6.3 Hydrogen production distribution

In the future hydrogen-demand base scenario, hydrogen is produced with a mix of technologies, not limited to the one production method. Significant cost and performance improvements make electrolysis emerge as the most attractive methods for hydrogen production in the long term. About 2.8 million tonnes, or approximately 65.95% of the hydrogen consumed, is produced by electrolysis, with 30 % (19.5 % of the total production) sent via the storage facilities prior to consumption. Moreover, hydrogen produced from natural gas also plays a significant role in the base case, constituting 34.05 % of the total supply. Production from SMR with CCS makes up the entire supply based on natural gas at 1.47 million tonnes. Interestingly, no import is seen from SMR without CCS, as the CO_2-cost tilt production in favour of SMR + CCS. As observed in Table 4.8 and 4.9, adding CCS

to SMR production results in an increase of 14.4 % the cost of H_2 per kg. Other studies have found CCS to increase the present levelised cost of hydrogen with and 18-100 % by adding CCS [22, 21]. An increase in cost estimates of CCS technology could potentially shift hydrogen production from natural gas to SMR without CCS.

The results are in contrast to a previous cost-optimisation study of the EU energy system, which finds that only when CO_2 storage was not possible, limiting the possibility of production from SMR with CCS, was electrolysis the main hydrogen production route [4]. Other studies find larger shares of electrolysis in 2050 [10], which highlight the difficulty of analysing future energy systems based on highly uncertain exogenous input factors, such as, fuel prices and cost of hydrogen production and renewable energy technologies.

Moving on, the distribution of the source of hydrogen vary between the system nodes, as depicted by Figure 5.7. Large demand nodes such as DE, NL and the UKs are supplied with hydrogen from both SMR and electrolysis, with the majority originating from the latter. The similar distributions can be observed in DK-E, DK-W, FI, IE and NI. These nodes also have significant portions of H_2 supplied via storage. Contrasting, the hydrogen production in the NO and SE nodes is sourced entirely from electrolysis with minimal storage use, which are all nodes with a significant share of installed hydropower in their capacity mix.

6.4 Hydrogen production cost

The optimisation returns a cost of hydrogen in the range of 1.57 - 2.6 €/kg depending on the node, with an unweighted average of 1.9 €/kg, as seen from Figure 5.8. Hydrogen produced at cost-levels in the lower part of the interval originates from the NO and SE nodes, where NO2 has the lowest H_2 price of the system at 1.57 €/kg. As found by [16], access to cheap and flexible hydropower lowers the cost of hydrogen in a system with larges shares of energy coming from VREs. A previous study, modelling hydrogen production in the European energy system, finds that hydropower facilitates increased full load hour operation of electrolysers, resulting in hydrogen costs around 2.0 €/tonne in NO and SE. The study indicates production costs between 2.5-3.0 €/kg in the UK, DE and NL, slightly above, but comparable to the results found [9]. As shown in Figure 5.7, these nodes have significant shares of hydrogen coming from SMR + CCS, and substantial investments in storage to compensate for a less flexible energy mix. BE imports about 85 % of the hydrogen demand from natural gas, effectively reaching the production cost of SMR with CCS, accounted for the price of CO_2. Interestingly, FI supply most of its demand from electrolysis without storage, while importing large quantities of electricity (mainly from SE1 and SE2), seen in Figure 5.5. As the model does not invest in storage capacity, FI is effectively subject to rationing penalties due to unserved demand in times of uneven electricity supply, heavily influencing the cost of hydrogen.

Other literature find systemic production costs in 2050 in ranges of 0.7-1.5 €/kg H_2 [8] to 2-5 €/kg [14], not considering price differences between different areas. These studies

use different modelling techniques, data inputs and assumptions, once more underlining the uncertainty associated with this type of analysis. Hydrogen production cost in a system with high RES shares are, for example, significantly exposed to changes in expected future CAPEX of the electrolyser and VRE technologies. Figure 5.16 and 5.17 shows the cost of hydrogen for variations in the mentioned CAPEX values in 2050. With a 100 % increase in CAPEX, 100 % of the hydrogen stems from SMR with CCS, as seen from Figure 5.14. This causes nodal prices, and thus the average costs, to converge towards approximately 2.6 €/kg H_2, which is the price of import from SMR with CCS. On the contrary, Figure 5.15 depicts that a 50 % CAPEX reduction amplifies electrolyser production and storage utilisation, reducing the nodal hydrogen price to 1.0 €/kg and the average price to 1.25 €/kg.

This project examines only the cost of centralised hydrogen production at the nodes, without considering transportation and other distribution-related costs. Several studies stress that the transmission costs of hydrogen can have a considerable effect on consumer costs, with variations between 0.1 - 3.5 €/kg depending on transportation method, distance and flow [14] [59]. It is emphasised that future technology development estimates are subject to a high degree of uncertainty, as hydrogen transmissions, as of today, is considered an immature segment. Nonetheless, the cost of transportation is highly influential to the competitiveness of hydrogen in the energy system. Hydrogen transmission can thus be worth investigating in further work.

6.5 Electrolyser and storage utilisation

Finally, in a system highly penetrated by RES, hydrogen from electrolysis becomes relevant to provide additional system flexibility to the energy system, acting as a flexible load.

The results depicted in Figure 5.2 show the possible output of electrolytic hydrogen for each node. Comparing these values to daily demand, the results clearly show that electrolysers are over-sized in terms of maximum output. For instance, DE can theoretically produce close to 8000 tonnes of H_2 a day, twice the daily demand. These findings are expected, as electrolyser utilisation at a constant maximum cannot be expected for a system largely penetrated by variable energy sources, leading to oversizing of production capacity. This is combined with the hydrogen storage investments shown in Figure 5.9, to provide hydrogen according to node requirements in a timely manner. As the hydrogen demand is assumed flat on a day-to-day basis, the storage option is essential for electrolyser operation flexibility. Figure 5.10 show how hydrogen storage levels in the nodal storage facilities fluctuate within the time span. Compared with the electricity generation mix in Figure 5.4, the results show how storage is used flexibly to store energy and supply hydrogen at times of high and low production from RES.

This flexibility, in addition to flexible import from SMR, results in a higher penetration of RES when comparing the energy production mixes for different hydrogen demands

seen in Figure 5.3 and 5.18. The development in emissions, net RES share and electricity curtailment for different hydrogen demands are summarised in Table 6.2 below.

Table 6.2: CO_2 emissions, net RES share and electricity curtailment for different hydrogen demands

H2 demand scaling from base	0	1	2	5
Net RES share	63.5 %	70.9 %	71.5 %	76.43 %
Curtailment	5.31 %	3.33 %	2.97 %	3.48 %
CO2 emissions [Million tonnes]	76.50	70.45	69.00	71.21

The system simulated without a hydrogen load has a net RES share of 63.5%, with curtailment of 5.3 % of the energy produced from variable RES. The RES share jump by more than 7 pp when the base hydrogen demand is introduced, further increasing with demand before reaching saturation at fives times the initial demand. Simultaneously, curtailment levels are reduced, indicating better utilisation of renewable assets in addition to increased renewable energy integration. The results are in accordance with previous research, which has found hydrogen penetration to effectuate integration and elevate RES shares [19, 20, 64]. In addition, [65] finds that the integration of hydrogen in the energy system also aids in reducing curtailment.

In addition, the results show that the larger penetration of renewable energy returns lower systemic CO_2 emissions, with levels decreasing from 76 million tonnes of CO_2 to 69 million tonnes with rising hydrogen demands, despite significant emissions related to the production of hydrogen from SMR with CCS. Although, emissions rise slightly at five times the base hydrogen demand, as many RES installation potentials are met, and the system must rely slightly more on SMR + CCS to supply the hydrogen load, as seen from Figure 5.19.

6.6 Implications of the CO_2 price

The cost of CO_2 heavily influences, as one would expect, generation from fossil-based power generation, seen in Figure 5.21. At zero carbon cost, coal and gas produce approximately 30 % of the energy. Coal has the largest emission-coefficient of the two, experiencing a rapid decline in share with increasing prices, until the complete phase-out at 60 €/t. CC gas sees a less steep decline, taking over from coal in this price area. This is approximately the price range where coal-to-gas switching is occurring in Europe today [64]. However, a switch from CC Gas to CCS Gas occurs at CO_2 price-level of 30 €/t, gradually increasing investments in CCS based generation and simultaneously decreasing generation from more conventional gas. This is largely in line with previous research, suggesting that CCS is introduced at substantial levels with prices in the 25–30 US$/t span, in most energy and economic modelling done to date [66]. Thus CCS prolongs the life of gas-based power production in a heavily carbon taxed system. Moreover, this thesis does not investigate the availability of CO_2 storage space, which is found by [4] be highly impactful on the composition of energy sources and sources of hydrogen. Available storage

space is assumed present but is however a restriction worth investigating in further work, as it can make or break the feasibility of CCS in the system.

The share of energy from renewable sources increases from 57 to 69 % with rising carbon costs. The market for generation based on renewable sources looks to be saturated in the 90-120 €/tonne CO_2-span, with the growth rate for wind power and solar converging towards zero. Effectuating a CO_2 price also has a significant effect on the CO_2-emissions from the electric power system and production of hydrogen. A substantial reduction is seen in Figure 5.22 at price levels between 30 and 60 €/t. Applying a CO_2 price of 60 €/t leads to the substitution of fossil sources with emission-less offshore wind and nuclear, consequently reducing CO_2 emission by 76 % compared to levels seen at no CO_2 costs. To further halve emissions, a large price increase to around 200 €/t CO_2 is required.

6.6.1 Hydrogen production and costs

The CO_2 price affects the hydrogen production composition in two ways, directly by influencing the emission-related costs of SMR and SMR with CCS, and indirectly by changing the energy mix, which influences electrolyser operation. The results in Figure 5.23 indicate that a carbon dioxide price in the 30-60 €/t-range is where hydrogen production from SMR is losing its edge to SMR with CCS. Hence, the results show that CCS is introduced in H_2 production at slightly higher price-levels compared to energy production. The loss of dispatchable power generation, and hence production flexibility, is compensated by a substantial increase in import from SMR between 0-60 €/t, from about 0.55 to 1.35 billion kgs of H_2.

The leading role, however, is played by electrolysis, for all costs of CO_2. Low prices encourage direct electrolysis, utilising RES in tandem with gas and coal, as seen by the spike in direct electrolysis production at no carbon dioxide cost in Figure 5.23. As a consequence, total electric energy production increases in Figure 5.20, while little storage is required. Higher levels of CO_2 costs encourages electrolysis with increased storage utilisation, rising to almost 30 pp of the H_2 production, to compensate for more expensive SMR imports and loss of dispatchable power generation.

Furthermore, the change in energy production and sources of hydrogen as a result of increasing CO_2 costs influence the cost of hydrogen produced in the system nodes. Overall, hydrogen production cost increase by 0.1-0.2 €/kg H_2 in the nodes depending on fossil electricity production or imports from natural gas to serve the hydrogen load. The hydropower nodes are mostly unaffected, as the average electricity price seen by electrolysis in Figure 5.25 is steady around 30 €/MWh, a level comparable to the prices seen in Scandinavia the past years [67], and with 100 % production based on electrolysis.

Nodes such as DE, IE, NI, NL, and the UKs experience a significant shift downwards from initial electricity prices slightly below 30 €/MWh, gradually increasing with rising CO_2 costs. The price of CO_2 impacts these nodes by reducing the financial competitiveness of fossil-based power generation, thus reducing its utilising in the energy mix, as seen in Figure 5.20. However, the figure still indicates shares of fossil-based power generation,

which produce at substantially elevated costs levels due to the price of carbon dioxide. Hence there are two factors affecting the price of electricity in opposite directions. It must be underlined that this price is not describing the levelised cost of electricity, but rather the market price seen by each node, which is influenced by several other factors, such as electricity exchange between nodes at different cost levels. Nonetheless, the sum of lower levels of power generation from natural gas, and the lower levels of hydrogen import from SMR with CCS seen in Figure 5.23, at a higher price, and increased investments in storage, lead to a slight increase of 0.1 €/kg H_2 for these nodes over the entire CO_2 price span.

To summarise, the cost of hydrogen production does not see detrimental effects of applying a price of CO_2, and remain at competitive levels when compared to previous discussions.

In conclusion, the CO_2 price is found to have a significant impact on the results, influencing the composition of energy-producing assets and sources of hydrogen in the system, largely in line with previous research on the matter [4, 65]. The hydrogen production price, however, is affected to a lesser extent. Moreover, the large share of electrolysis, even at low levels of CO_2 costs, suggest that other factors are more influential in determining the economic parity between electrolytic and SMR based H_2. Overall, policymakers aiming to decarbonise the European economy should adopt stringent CO_2 tax levels, both to increase the share of energy production from - and to provide hydrogen based on low-carbon sources.

6.7 Implications of the price of natural gas

6.7.1 Energy generation

The results indicate that the price of natural gas is highly influential on the energy generation mix, observed in Figure 5.26 and 5.28. The relative change in the financial viability of power generation from natural gas caused by the change in the fuel price leads to a large span in the level of CC gas deployment, regardless of CO_2 price level. The cost parity between natural gas and coal seems to lie around the base case natural gas price with no CO_2 price, with generation from coal expanding heavily beyond this point in Figure 5.28. A CO_2 price of 60 €/tonne makes coal completely uneconomical until gas prices rise by 30 % from base, when it is used to compensate for the loss of dispatchable gas generation in tandem with nuclear and biomass. As discussed, CCS is utilised at a CO_2 cost above 30 €/t. CCS is not economically viable, and obviously unnecessary from an economic stand-point, with costs at 0 €/t, and as a result not deployed regardless of the price of natural gas. However, at a CO_2 price of 60 €/t and reducing natural gas prices, CCS gas deployment increase to a share of approximately 10 % of the total energy produced.

6.7.2 Influence on the hydrogen production mix

The deployment of hydrogen production from SMR is, as could be expected, heavily dependant on the gas price, as it constitutes the significant portion of the production costs. Figure 5.30 shows that supply from SMR with CCS decreases linearly with the natural gas price, substituted by electrolysis and storage. The storage growth rate is more substantial compared to electrolysis, as seen by the slope in Figure 5.31, suggesting loss off dispatchable generation and the flexibility of SMR import is balanced with hydrogen storage, and that flexibility and dispatch capabilities are necessary for large-scale hydrogen production from renewable sources. The results also indicate that electrolytic- and SMR with CCS-based hydrogen are of an approximately equal share in the hydrogen production mix at a 30 % reduction in natural gas prices, suggesting price parity between the two at these levels for the given CO_2 price. Further declines expand SMR utilisation to approximately 60 % of the total hydrogen produced. Several studies have found SMR-based hydrogen to be the favourable production method [4, 14, 68], and the results showcase the influence of which fuel and CO_2 has on its deployment in a future low-carbon power system.

Moreover, interesting results are observed from Figure 5.32 when running the simulation for varying natural gas prices at no CO_2 cost. When prices are halved, 65 % of the hydrogen production stem from electrolysis, contrasting previous results where the larger portion came from hydrogen sourced from SMR with CCS at 60€/tonne of CO_2. From Figure 5.33 it can be observed that DE, DK-E, DK-W, FI, IE, NI, UK-S, and even NL, one of the three SMR hubs with no hydrogen transportation costs, produce 100 % of the hydrogen by electrolysis. What these nodes have in common are large shares of CC gas capacity initially installed, which experiences a substantial rise in utilisation and share of the total energy produced, seen in Figure 5.28, for declining gas prices. The only investments are in electrolyser capacity for the mentioned nodes. This indicates that electrolysis powered by CC gas is, in fact, more economical than producing H_2 via SMR at low gas prices and no CO_2 cost. On the contrary, the hydropower nodes import their entire hydrogen demand from SMR at low gas prices, before switching to electrolysis between a price scaling of 0.7 and 0.8.

For increasing natural gas prices at no CO_2 cost, a significant increase in H_2 imported from SMR is observed initially in 5.32, before gradually declining with rising prices. In this interval, power generation from natural gas is approximately halved, without a similar growth in other energy sources. Coal is expanding massively from 1.1 and on-wards, providing more dispatchable generation, but still at insufficient levels to equalise the loss of generation from CC gas. Consequently, storage capabilities are slightly strengthened and H_2 from natural gas imports sees an upsurge. While natural gas pricing influences both the cost of power generation and hydrogen production from natural gas, the variable costs related to power generation are almost exclusively attributable to feedstock pricing. Differences in efficiencies, fuel usage, and cost compositions seem to make power production from NG more exposed to fluctuations price compared to SMR. Consequently, SMR is relatively cheaper to power generation at increased price levels and vice versa at low prices. This can also be a result of the indirect modelling of production from SMR, as costs are scaled without considering the size and output of the plant. Direct modelling of

SMR would allow for a more dynamic response to changing market conditions and provide more realistic results. Such a modelling task is, however, out of the scope and time-limit of this thesis. Nonetheless, the results given are expected to be of sufficient precision for this purpose.

Furthermore, Figure 5.29 shows the importance of balance in pricing in the commodities market for the future system from an emissions-perspective. As previously discussed, low prices encourage import of hydrogen from SMR without CCS and electrolysis powered by gas. On the contrary, natural gas prices at too high levels facilitate the use of coal to make up for lost production flexibility. The environmental optimum seems to lie in the middle of the two.

In terms of hydrogen costs, the results in Figure 5.34 indicate that the future competitiveness of low-carbon hydrogen is highly dependent on gas prices. At low NG price levels, all nodes experience a hydrogen price around 1.3 €/kg, comparable to the hydrogen costs from SMR expected in Europe today at 1.5 €/kg [14]. The cost of hydrogen grows linearly with the NG price, until the NO and SE nodes switch to hydropower, consequently decoupling H_2 production costs from the price of natural gas. Costs continue to rise in the remaining nodes, as some hydrogen from SMR is imported regardless of NG price level. This shows that nodes without sufficient alternatives to flexible power- and hydrogen production are unable to decouple entirely from fossil sources, despite significant storage installation.

In conclusion, natural gas prices are a decisive factor when considering the future hydrogen production mix and emissions, as it heavily influences both hydrogen directly produced from SMR, with and without CCS, and gas-powered electricity generation and thus the future energy mix. The results indicate that hydrogen from steam methane forming of natural gas has a role, to some extent, in a future decarbonised energy system regardless of fuel prices and CO_2 costs, where it can provide hydrogen when production conditions for low carbon sources are unfavourable.

6.8 Method and scenario shortcomings

There are several shortcomings with the modelling approach, input data and assumptions used to create the optimisation model and base scenario for this master's thesis.

Firstly, the use of linear programming with continuous decision variables allows the capacity expansion decisions to be continuous. This opens up for the decision variables to be fractional, meaning, for example, the model can invest in half a power plant, scaling the size of an asset linearly without restriction. This can be a valid assumption in many cases, such as producing one-third of a kilo hydrogen, not restricted to increments of a whole kilo. On the contrary, investing in half a gas power plant with CCS is more questionable, as this expansion is realistically binary, and one either invest or not. Moreover, CAPEX and fixed costs of such an investment do not necessarily follow capacity increases linearly, as expanding a thermal power plant might require investments in a new turbine

or upgrades of a transformer, which are usually upgraded in bulks, not linearly with each MW expanded. Applying a integer programming model, on the other hand, would accommodate this problem, only allowing for variables of integer quantities. This would likely increase the total costs of the system, as the model would be required to invest in, for example, 50 MW of coal at minimum, while only 30 MW is needed to fulfil load requirements. On the contrary, such investments would allow for considerations of economies of scale, lowering the annual costs. However, employing non-linear programming can significantly increase computational time [69], and require data processing capacity outside of what is at the disposal of this work. Consequentially, a smaller system and more approximations might be required, and it is uncertain whether strict integer commitments would generate significantly better results.

Secondly, way of modelling thermal power plant ramping, as seen in Equation 3.15, linearises the operation of the power plants. This opens up to power plants altering their production at a rate exceeding what is technically possible, and the capabilities of, for example, CC gas, to provide power system flexibility may be overestimated, thus affecting expansion and utilisation of storage and electrolysers. Nonetheless, the model outcome is not significantly influenced by this detail, given the production level- and ramping restrictions.

Lastly, there are other notable shortcomings related to the model input and assumptions, not discussed in previous sections. The low geographical resolution applied in the system investigated entails aggregation of data sets for entire countries into single or a few system nodes. The production profiles used to describe VRE operation are aggregated over large geographical areas into, for example, a single node in Germany. As parts of DE can experience significant wind while other parts may be windless, aggregating the input profiles into one node will smooth production variability, resulting in less realistic VRE asset operation, as highlighted by [63]. This aggregation also means that transmission congestions within a large area are neglected, which could significantly influence the flow of power and other model output. Moreover, data sets for only one specific climatic year is applied, meaning that variability in various conditions between years is neglected, making the temporal resolution of this study somewhat inadequate. Furthermore, the hydrogen demand is modelled as constant on a day-to-day basis in each node. At the same time, consumption patterns may be influenced by, for example, weather, cost of substitutes and other macroeconomic factors. However, due to the present absence of a widespread and large-scale market for hydrogen and lack of actual hydrogen load data sets, this approximation is assumed sufficient for the purpose of this work. In addition, this thesis only considers battery storage and hydrogen storage in tanks. Including more storage options in the analysis, such as hydrogen storage in salt caverns or saline aquifers, pumped hydro or compressed-air storage would provide even more flexibility options to the system, which could further elevate the share of RES in the energy mix. This could also potentially result in reduced utilisation of electrolysers and hydrogen storage to provide system flexibility.

Chapter 7

Conclusion and further work

7.1 Conclusion

This master's thesis investigates a system of selected of countries in North-Western Europe, divided into system nodes in 2050, utilising a state-of-the-art capacity expansion optimisation model based on linear programming, to analyse the effects of large-scale integration of hydrogen into an interconnected multiple energy-carrier energy system. The model optimises investments in power generation capacities, electrolysers, hydrogen import from natural gas reforming coupled with pipeline transport and the option for CCS, electric and hydrogen energy storage, and electricity exchange between nodes, to find the best pathways of producing hydrogen and supplying nodal electricity and hydrogen consumption at least cost.

The results show that hydrogen produced from electrolysis is the main production pathway, providing 65 % of the hydrogen consumed in the base case scenario. High storage utilisation is found, as 30 % of the electrolytic hydrogen is transported via storage prior to consumption, except for nodes with large hydropower capacities, which utilise hydropower flexibility to produce hydrogen from electrolysis directly. The remaining share of H_2 is supplied by SMR with CCS, as the price of carbon dioxide favours this pathway over SMR without CCS.

Moreover, the results show that the onshore and offshore wind power is the most significant contributors to the electricity production mix in the system in 2050, based on expected future technology cost reductions. In accordance with similar studies, the flexibility provided by the integration of hydrogen production and storage into the energy system increases power system penetration of variable renewable energy. The base case simulated without hydrogen production integrated has a net renewable share of the 63.5 %, increasing to 70.9 % with the deployment of hydrogen production, further rising to 76.43 % at

greater hydrogen load levels.

Furthermore, the optimisation model calculates a marginal price of hydrogen in the span of 1.57 to 2.6 €/kg for the system nodes. It is found that future VRE and electrolyser technology CAPEX estimates are highly influential on the cost of hydrogen and composition of H_2 sources, reducing the price as low as 1.0 €/kg and elevating electrolysis utilisation for a 50 % CAPEX reduction. On the contrary, SMR with CCS supplies the entire hydrogen load at an average price of 2.6 €/kg, when CAPEX estimates are increased by 100 % .

Among the other insights developed from the results is that the deployment of a carbon dioxide price has a considerable effect on the future energy system. A price of 30 €/t CO_2 is found to both effectuate coal phase-out and introduce CCS based power generation, which lead to substantial system emission reductions, while not affecting the hydrogen production cost more than 0.1-0.2 €/kg. Increasing prices beyond 90-120 €/t CO_2 does not lead to increased RES in the energy mix. The 30-60 €/t CO_2 price span also triggers a switch from grey to blue hydrogen. However, electrolysis is the dominant production technology for all price ranges.

Natural gas prices are also found to highly influential of the future electricity and hydrogen production mix. The cost parity between coal and combined-cycle gas is found at the base case natural gas price of 11.5 MMBtu, neglecting CO_2 prices. A decrease in the price of 50 % results in fossil energy share of 38 %, and 22 % at 60 €/t CO_2. Electrolysis is the favoured production pathway, despite the change in prices of natural gas from these levels, as low gas prices facilitate electrolysis powered by natural gas generation. A 30 % reduction in the base case natural gas price, with a CO_2 price of 60 €/t, is found as the price parity level between hydrogen produced from electrolysis and SMR with CCS, with further reductions leading the latter hydrogen pathway to dominate. Additionally, the cost of hydrogen increase from a united system price 1.2 €/kg to a price span of 1.55-2.2 €/kg H_2 with gas price variations of -+ 50 %, and it is highlighted that some natural gas is utilised in the system regardless of natural gas price levels.

It is highlighted that input data and method can significantly impact model output. The capacity expansion is conducted with VRE profiles based on single-year data, and the areas subject to analysis are aggregated into single or few nodes, neglecting variations in production conditions between years and local power system dynamics. In further works, this study should be complemented with research of higher spatial and temporal resolution to increase result robustness. Moreover, additional hydrogen production and storage methods should be added to give a broader assessment of pathways for hydrogen from low carbon sources. Lastly, the model is implemented as a linear programming optimisation model, which allows for somewhat unrealistic continuous investment decisions in power generation capacities. Other programming approaches should thus be investigated to assess the impact on the results.

7.2 Further work

Objectives of further work can be:

- Run the system for multiple climatic years to identify the impact of the production profile inputs
- Investigate a more complete system, considering costs and losses related to electricity transfer and storage in-between production and transportation, to provide more realistic results.
- Investigate other transportation methods, such as, natural gas, ammonia and methanol.
- Run the model for a system based entirely on low carbon sources to investigate implications of a zero-emission energy system
- Expand the optimisation model to include a larger European energy system
- Investigate distribution from the hub to the end user in order to calculate the nozzle price of hydrogen.
- Expand the system to include other energy storage and hydrogen production pathways
- Add the option to supply the system with power from fuel cells and hydrogen storage to investigate buffer capabilities

Bibliography

[1] European Commission. COMMUNICATION FROM THE COMMISSION - The European Green Deal, Dec 2019. Brussels. COM/2019/640 https://ec.europa.eu/info/strategy/priorities-2019-2024/european-green-deal_en [Online; accessed 3. Jun. 2020].

[2] O. V. Marchenko and S. V. Solomin. The future energy: Hydrogen versus electricity. *Int. J. Hydrogen Energy*, 40(10):3801–3805, Mar 2015. doi: 10.1016/j.ijhydene.2015.01.132.

[3] Shell. *Shell Hydrogen study - Energy of the future?*, Dec 2017. Shell Deutschland Oil GmbH. https://www.shell.com/energy-and-innovation/new-energies/hydrogen.html. [Online; accessed 13. Apr. 2020].

[4] Herib Blanco, Wouter Nijs, Johannes Ruf, and André Faaij. Potential for hydrogen and Power-to-Liquid in a low-carbon EU energy system using cost optimization. *Appl. Energy*, 232:617–639, Dec 2018. doi: 10.1016/j.apenergy.2018.09.216.

[5] Jørg Aarnes, Marcel Eijgelaar, and Erik A. Hektor. *Hydrogen as an energy carrier*, 2018. DNV GL. https://www.dnvgl.com/oilgas/download/hydrogen-as-an-energy-carrier.html. [Online; accessed 16. May 2020].

[6] European Commission. Clean energy - an EU Hydrogen Strategy, Mar 2020. https://ec.europa.eu/info/law/better-regulation/have-your-say/initiatives/12407-A-EU-hydrogen-strategy [Accessed 26. Mar. 2020].

[7] Marius Moldestad. *Evaluating transport pathways for hydrogen produced from low-carbon energy sources*, Des 2019. [Project thesis. Norwegian University of Science and Technology].

[8] F.Wouters A.J.M van Wijk. *Green Hydrogen for a European Green Deal - A 2x40 GW Initiative*, March 2020. Brussels, Belgium.

https://www.hydrogen4climateaction.eu/2x40gw-initiative
[Online; accessed 28. May 2020].

[9] K. Kanellopoulos and H. Blanco Reano. *The potential role of H2 production in a sustainable future power system*, Mar 2019. Publications Office of the European Union. https://ec.europa.eu/jrc/en/publication/potential-role-h2-production-sustainable-future-power-system. [Online; accessed 7. Apr. 2020].

[10] Fuel Cells and Hydrogen Joint Undertaking. *Hydrogen roadmap Europe:A sustainable pathway for the European energy transition*, Jan 2019. [Luxembourg. Bietlot] https://www.fch.europa.eu/news/hydrogen-roadmap-europe-sustainable-pathway-european-energy-transition.

[11] Kjetil Malkenes Hovland. Statkraft og stålprodusent med klimagrep: Vil lage stål med hydrogen. *E24*, Jun 2020.
https://e24.no/olje-og-energi/i/VbmEBr/statkraft-og-staalprodusent-med-klimagrep
[Online; accessed 3. Jun. 2020].

[12] Thema Consulting Group. *Systemvirkninger og næringsperspektiver ved hydrogen*, May 2019. https://www.thema.no/wp-content/uploads/2019/05/THEMA-rapport-2019-07-Systemvirkninger-og-n%C3%A6ringsperspektiver-ved-hydrogen.pdf [Online; accessed 16. May 2020].

[13] Gas for Climate and Guidehouse. *Gas Decarbonisation Pathways 2020-2050*, April 2020. https://gasforclimate2050.eu/publications/.
[Online; accessed 19. May. 2020].

[14] IEA. *The Future of Hydrogen*, Dec 2019. https://www.iea.org/reports/the-future-of-hydrogen
[Online; accessed 6. Jun. 2020].

[15] Klaus Skytte. The regulating power market on the Nordic power exchange Nord Pool: an econometric analysis. *Energy Economics*, 21(4):295–308, 8 1999.
doi: 10.1016/S0140-9883(99)00016-X.

[16] Espen Flo Bødal and Magnus Korpås. *Value of hydro power flexibility for hydrogen production in constrained transmission grids*. *International Journal of Hydrogen Energy*, 5 2019.
doi: 10.1016/J.IJHYDENE.2019.05.037.

[17] Mehdi Jafari, Magnus Korpås, and Audun Botterud. Power system decarbonization: Impacts of energy storage duration and interannual renewables variability. *Renewable Energy*, 156:1171–1185, Aug 2020.
doi: 10.1016/j.renene.2020.04.144.

[18] Herib Blanco and André Faaij. A review at the role of storage in energy systems with a focus on Power to Gas and long-term storage. *Renewable Sustainable Energy Rev.*, 81:1049–1086, Jan 2018.
doi: 10.1016/j.rser.2017.07.062.

[19] M. Korpas and A. T. Holen. Operation planning of hydrogen storage connected to wind power operating in a power market. *IEEE Trans. Energy Convers.*, 21(3):742–749, Aug 2006.
doi: 10.1109/TEC.2006.878245.

[20] Christopher J. Greiner, Magnus Korpås, and Terje Gjengedal. Dimensioning and operating wind-hydrogen plants in power markets. *12th WSEAS International Conference on CIRCUITS*, July 2008.
https://www.researchgate.net/publication/261861418_Dimensioning_and_operating_wind-hydrogen_plants_in_power_markets.

[21] Yaser Khojasteh Salkuyeh, Bradley A. Saville, and Heather L. MacLean. Techno-economic analysis and life cycle assessment of hydrogen production from natural gas using current and emerging technologies. *Int. J. Hydrogen Energy*, 42(30):18894–18909, Jul 2017.
doi: 10.1016/j.ijhydene.2017.05.219.

[22] IEA. *Techno - Economic Evaluation of SMR Based Standalone (Merchant) Hydrogen Plant with CCS*, February 2017. http://ieaghg.org/exco_docs/2017-02.pdf. [Online; accessed 6. Jun. 2020].

[23] S. Shiva Kumar and V. Himabindu. Hydrogen production by PEM water electrolysis – A review. *Mater. Sci. Energy Technol.*, 2(3):442–454, Des 2019.
doi: 10.1016/j.mset.2019.03.002.

[24] Saba et al. The investment costs of electrolysis – A comparison of cost studies from the past 30 years. *Int. J. Hydrogen Energy*, 43(3):1209–1223, Jan 2018.
doi: 10.1016/j.ijhydene.2017.11.115.

[25] Stiller et al. Options for CO2-lean hydrogen export from Norway to Germany. *Energy*, 33(11):1623–1633, Nov 2008.
doi: 10.1016/j.energy.2008.07.004.

[26] Omar J. Guerra, Joshua Eichman, Jennifer Kurtz, and Bri Mathias Hodge. Cost Competitiveness of Electrolytic Hydrogen. *Joule*, 3(10):2425–2443, 7 2019.
doi: 10.1016/j.joule.2019.07.006.

[27] Jan Lundgren, Mikael Rönnqvist, and Peter Värbrand. *Optimization*, 2010.
Edition 1:2.
Lund. Holmberg.

[28] Toufik Sebbagh, Ridha Kelaiaia, Abdelouahed Assia, and Abdelouahab Zaatri. Optimizing the use of green energies, an application to crop irrigation. 12:87–98, 08 2018.
https://www.researchgate.net/publication/327022560_Optimizing_the_Use_of_Green_Energies_an_Application_to_Crop_Irrigation.

[29] Gagnon, Pieter, Galen Barbose, Brady Stoll, Ali Ehlen, Jarrett Zuboy, Trieu Mai, and Andrew Mills. 2018. *Estimating the Value of Improved Distributed Photovoltaic Adoption Forecasts for Utility Resource Planning.* NREL/TP-6A20-71042, Golden,

CO: National Renewable Energy Laboratory; Berkeley, CA: Lawrence Berkeley National Laboratory.
https://www.nrel.gov/docs/fy18osti/71042.pdf
[Online; accessed 3. Jun. 2020].

[30] Benjamin Pfluger. *Assessment of least-cost pathways for decarbonising Europe's power supply : a model-based long-term scenario analysis accounting for the characteristics of renewable energies*, May 2013. PhD thesis. Karlsruher Institut für Technologie.

[31] Martin Kristiansen, Harald G. Svendsen, Magnus Korpås, and Stein-Erik Fleten. Multistage grid investments incorporating uncertainty in offshore wind development. *Energy Procedia*, 137:468–476, Oct 2017.
doi: 10.1016/j.egypro.2017.10.371.

[32] Martin Kristiansen, Magnus Korpås, and Hossein Farahmand. Economic and environmental benefits from integrated power grid infrastructure designs in the North Sea. *J. Phys. Conf. Ser.*, 1104(1):012034, Oct 2018.
doi: 10.1088/1742-6596/1104/1/012034.

[33] Dirk Van Hertem, Jody Verboomen, K. Purchala, Ronnie Belmans, and W.L. Kling. Usefulness of DC power flow for active power flow analysis with flow controlling devices. *Studies in Surface Science and Catalysis - STUD SURF SCI CATAL*, pages 58 – 62, 04 2006. https://www.researchgate.net/publication/4243438_Usefulness_of_DC_power_flow_for_active_power_flow_analysis_with_flow_controlling_devices.

[34] Magnus Korpås and Espen Flo Bødal. *Integration of renewables in large-scale hydrogen production*, Dec 2019. https://www.sintef.no/globalassets/project/hyper/presentations-day-1/day1_1330_korpas_ntnu.pdfl [Online; accessed 18. Jun. 2020].

[35] Python.org. *Python*. https://www.python.org.
[Online; accessed 18. Jun. 2020].

[36] William E. Hart, Jean Paul Watson, and David L. Woodruff. Pyomo: Modeling and solving mathematical programs in Python. *Mathematical Programming Computation*, 3(3):219–260, 2011.
doi: 10.1007/s12532-011-0026-8.

[37] William E Hart, Carl D Laird, Jean-Paul Watson, David L Woodruff, Gabriel A Hackebeil, Bethany L Nicholson, and John D Siirola. *Optimization Modeling in Python - Springer Optimization and Its Applications*, volume 67. 2017.
doi: 10.1007/978-3-319-58821-6.

[38] Gurobi.com. *Gurobi - The fastest solver*. https://www.gurobi.com.
[Online; accessed 18. Jun. 2020].

[39] North Pool. Bidding areas.
https://www.nordpoolgroup.com/the-power-market/Bidding-areas
[Online; accessed 5. May 2020].

[40] L. Riboldi, S. Völler, M. Korpås, and L.O Nord. An Integrated Assessment of the Environmental and Economic Impact of Offshore Oil Platform Electrification. *Energies* 2019. 12. 2114.
https://doi.org/10.3390/en12112114.

[41] Klaus Stratmann. Germany's north-south divide, Jun 2016. *Handelsblatt*
https://www.handelsblatt.com/today/politics/handelsblatt-exclusive-germanys-north-south-divide/23537748.html?ticket=ST-2967631-ofEAwBf1IBmu6BrVryQi-ap4
[Online; accessed 5. May 2020].

[42] European Commission. *EU Reference Scenario 2016 - energy, transport and GHG emission trends to 2050*, August 2016. https://ec.europa.eu/energy/sites/ener/files/documents/20160713%20draft_publication_REF2016_v13.pdf. [Online; accessed 19. Apr. 2020].

[43] NTSO-E. *Ten-Year Network Development Plan 2010–2020.*, Jun 2010. https://eepublicdownloads.blob.core.windows.net/public-cdn-container/clean-documents/pre2015/SDC/TYNDP/TYNDP-final_document.pdf. [Online; accessed 11. Apr. 2020].

[44] Paul Breeze. Combined Cycle Power Plants. *Gas-Turbine Power Generation*, pages 65–75, Jan 2016.
doi: 10.1016/B978-0-12-804005-8.00007-0.

[45] A. Crosara, E. Tómasson, and L. Söder. Generation adequacy in the nordic and baltic area: The potential of flexible residential electric heating. In *2019 IEEE PES Innovative Smart Grid Technologies Europe (ISGT-Europe)*, pages 1–5, 2019.
https://ieeexplore.ieee.org/document/8905720.

[46] European Commission. *Hydrogen use in EU decarbonisation scenarios*, Feb 2020. https://ec.europa.eu/jrc/sites/jrcsh/files/final_insights_into_hydrogen_use_public_version.pdf. [Online; accessed 10. Apr. 2020].

[47] Idealhy. *Liquid Hydrogen Outline*, 2020. https://www.idealhy.eu/index.php?page=lh2_outline. [Online; accessed 10. Apr. 2020].

[48] National Renewable Energy Laboratory (NREL). *2019 Annual Technology Baseline: Electricity*, 2019.
https://atb.nrel.gov/
[Online; accessed 24. Apr. 2020].

[49] XE. *XE Currency Converter: 1 EUR to USD*.
https://www.xe.com/currencyconverter/convert/?Amount=1&From=EUR&To=USD
[Online; accessed 27. Mar. 2020].

[50] IEA. *World Energy Outlook 2016*, 2016.
International Energy Agency. Paris, France. https://www.iea.org/reports/world-energy-outlook-2016. [Online; accessed 19. Apr. 2020].

[51] National Renewable Energy Laboratory (NREL). H2A: Hydrogen Analysis Production Case Studies - Hydrogen and Fuel Cells - NREL, 2019. https://www.nrel.gov/hydrogen/h2a-production-case-studies.html.
[Online; accessed 4. May. 2020].

[52] Eurostat. *Natural gas supply statistics*, 2020. https://ec.europa.eu/eurostat/statistics-explained/index.php?title=Natural_gas_supply_statistics&oldid=447636#Supply_structure. [Online; accessed 27. Apr. 2020].

[53] Michelle Bentham and Mg Kirby. Co 2 storage in saline aquifers. *Oil Gas Science and Technology-revue De L Institut Francais Du Petrole - OIL GAS SCI TECHNOL*, 60:559–567, 05 2005.
doi: 10.2516/ogst:2005038.

[54] Michael Godec, Vello Kuuskraa, Tyler Van Leeuwen, L. Stephen Melzer, and Neil Wildgust. CO2 storage in depleted oil fields: The worldwide potential for carbon dioxide enhanced oil recovery. *Energy Procedia*, 4:2162–2169, Jan 2011.
doi: 10.1016/j.egypro.2011.02.102.

[55] Sarah Hannis, Jiemin Lu, Andy Chadwick, Sue Hovorka, Karen Kirk, Katherine Romanak, and Jonathan Pearce. CO2 Storage in Depleted or Depleting Oil and Gas Fields: What can We Learn from Existing Projects? *Energy Procedia*, 114:5680–5690, Jul 2017.
doi: 10.1016/j.egypro.2017.03.1707.

[56] Anne-Kari Furre, Ola Eiken, Håvard Alnes, Jonas Nesland Vevatne, and Anders Fredrik Kiær. 20 Years of Monitoring CO2-injection at Sleipner. *Energy Procedia*, 114:3916–3926, Jul 2017.
doi: 10.1016/j.egypro.2017.03.1523.

[57] National Renewable Energy Laboratory (NREL). *Future Central Hydrogen from Natural Gas without CO2 Capture and Sequestration*, Feb 2018. [NREL Excel model: www.nrel.gov].

[58] National Renewable Energy Laboratory (NREL). *Future Central Hydrogen from Natural Gas with CO2 Capture and Sequestration*, Feb 2018. [NREL Excel model: www.nrel.gov].

[59] Christopher Yang and Joan Ogden. Determining the lowest-cost hydrogen delivery mode. *Int. J. Hydrogen Energy*, 32(2):268–286, Feb 2007.
doi: 10.1016/j.ijhydene.2006.05.009.

[60] F.Wouters A.J.M van Wijk. *Hydrogen: The bridge between Africa and Europe*, Sep 2019. http://profadvanwijk.com/wp-content/uploads/2019/

09/Hydrogen-the-bridge-between-Africa-and-Europe-5-9-2019.pdf.
[Online; accessed 1. May 2020].

[61] Google. *Google Maps*, 2020.
https://www.google.com/maps
[Online; accessed 13. May. 2020].

[62] Yonas Gebrekiros. *Analysis of Integrated Balancing Markets in Northern Europe under Different Market Design Options*, 2015. PhD thesis. Norwegian University of Science and Technology.

[63] Martin Kristiansen. *Multinational transmission expansion planning: Exploring engineering-economic decision support for a future North Sea Offshore Grid*, 2019. PhD thesis. Norwegian University of Science and Technology.

[64] Schalk Cloete and Lion Hirth. Flexible power and hydrogen production: Finding synergy between CCS and variable renewables. *Energy*, 192:116671, Feb 2020.
doi: 10.1016/j.energy.2019.116671.

[65] Alessandra Sgobbi, Wouter Nijs, Rocco De Miglio, Alessandro Chiodi, Maurizio Gargiulo, and Christian Thiel. How far away is hydrogen? Its role in the medium and long-term decarbonisation of the European energy system. *Int. J. Hydrogen Energy*, 41(1):19–35, Jan 2016.
doi: 10.1016/j.ijhydene.2015.09.004.

[66] B. Metz, O. Davidson, H. de Coninck, M. Loos, and L. Meyer. IPCC. *Special Report on Carbon Dioxide Capture and Storage.* , 2005. Cambridge University Press.
https://www.ipcc.ch/site/assets/uploads/2018/03/srccs_chapter8-1.pdf
[Online; accessed 25. May. 2020].

[67] Nordpool. Day-ahead prices. https://www.nordpoolgroup.com/Market-data1/Dayahead/Area-Prices/ALL1/Yearly/?view=table. [Online; accessed 9. Jun. 2020].

[68] L. Barreto, A. Makihira, and K. Riahi. The hydrogen economy in the 21st century: a sustainable development scenario. *Int. J. Hydrogen Energy*, 28(3):267–284, Mar 2003.
doi: 10.1016/S0360-3199(02)00074-5.

[69] Duan Li and Xiaoling Sun. *Nonlinear Integer Programming*, 2006.
Edition 1:2.
New York, USA. Springer Science and Business Media LLC.

Appendix A

Appendix

A.1

$$Net\,RES\,share = \frac{Generation\,from\,RES - total\,curtailment}{Total\,amount\,of\,electricity\,generated} \tag{A.1}$$

$$CRF = \frac{i \cdot (1+i)^n}{(1+i)^n - 1} \tag{A.2}$$

$$AIC\,[EUR] = (PC\,[GW] \cdot L\,[km] \cdot InvCost\,[EUR/GW/km]) \cdot CRF + O\&M[EUR/yr] \tag{A.3}$$

$$LCOT\,[EUR/kg] = \frac{AIC\,[EUR]}{PC\,[GW] \cdot LF\,[hr/yr] \cdot HHV\,[GWh/kg} \tag{A.4}$$

Table A.1: Final energy demand and hydrogen demand for each node in 2050

Bus	Final energy demand [TWh]	Hydrogen demand [TWh]	Hydrogen demand [Tonnes/day]
BE	108	9.2	839
DE	580	49.3	4323
DK-E	18	1.5	139
DK-W	27	2.3	207
FI	96	8.2	746
IE	34	2.9	263
NI	10	0.8	74
NL	133	11.3	1031
NO1	41	3.5	320
NO2	25	2.1	194
NO3	24	2.0	185
NO4	20	1.7	152
NO5	20	1.7	152
SE1	10	0.8	75
SE2	22	1.9	170
SE3	103	8.7	798
SE4	31	2.7	244
UK-N	44	3.7	340
UK-M	175	14.9	1360
UK-S	219	18.6	1700

Table A.2: Various technology input parameters for 2050 [48]

Type	CO2 emission [kg/MWh]	Min. generation limit [MW]	Ramp rate [%/h]	Retirement costs [€/MW]
Onshore Wind	0	0	100 %	
Solar	0	0	100 %	
CT Gas	481.6	0	100 %	16993
CC Gas	333	0	25 %	12064
CCS Gas	39.8	0	25 %	31116
Coal	834.7	260	16 %	61025
CCS Coal	88.4	325	16 %	61025
Nuclear	0	2200	16 %	76440
Biomass	0	34	32 %	56987
Offshore Wind	0	0	100 %	

Table A.3: Transmission line capacities and connections between the system nodes in 2050 [40]

From	To	Capacity [MW]
NO1	NO2	1450
NO1	NO5	4100
NO1	NO3	1000
NO1	SE3	2920
NO2	UK-M	1400
NO2	NO5	2100
NO2	NL	700
NO2	DE	3500
NO2	DK-W	1640
NO3	NO5	1000
NO3	NO4	3000
NO3	SE2	1000
NO4	FI	50
NO4	SE1	650
NO4	SE2	275
NO4	UK-N	2000
SE1	FI	1150
SE1	SE3	3750
SE2	SE3	7650
SE3	SE4	5575
SE3	FI	1850
SE3	DK-W	710
SE4	DK-E	1500
SE4	DE	965
DK-W	DE	3000
DK-W	DK-E	1200
DK-W	NL	700
DK-W	UK-S	1400
DK-E	DE	1600
DE	NL	5000
DE	BE	1000
NL	UK-S	1000
BE	UK-S	1000
UK-N	NI	1000
UK-N	UK-M	7000
UK-M	IE	4400
UK-M	UK-S	15000
IE	NI	1100
BE	NL	2400

Marius Moldestad

NTNU
Norwegian University of
Science and Technology